Cold-Adapted Protein Kinases and Thylakoid Remodeling Impact Energy Distribution in an Antarctic Psychrophile[1]

Beth Szyszka-Mroz,[a,2] Marina Cvetkovska,[a,2,3] Alexander G. Ivanov,[a,b] David R. Smith,[a] Marc Possmayer,[a] Denis P. Maxwell,[a] and Norman P.A. Hüner[a,4,5]

[a]Biology Department and the Biotron Centre for Experimental Climate Change Research, University of Western Ontario, London, Canada N6A 5B7

[b]Institute of Biophysics and Biomedical Engineering, Bulgarian Academy of Sciences, Acad. G. Bonchev Str. bl. 21, 1113 Sofia, Bulgaria

ORCID ID: 0000-0001-8723-6961 (N.P.A.H.).

The Antarctic psychrophile *Chlamydomonas* sp. UWO241 evolved in a permanently ice-covered lake whose aquatic environment is characterized not only by constant low temperature and high salt but also by low light during the austral summer coupled with 6 months of complete darkness during the austral winter. Since the UWO241 genome indicated the presence of *Stt7* and *Stl1* protein kinases, we examined protein phosphorylation and the state transition phenomenon in this psychrophile. Light-dependent [γ-^{33}P]ATP labeling of thylakoid membranes from *Chlamydomonas* sp. UWO241 exhibited a distinct low temperature-dependent phosphorylation pattern compared to *Chlamydomonas reinhardtii* despite comparable levels of the Stt7 protein kinase. The sequence and structure of the UWO241 Stt7 kinase domain exhibits substantial alterations, which we suggest predisposes it to be more active at low temperature. Comparative purification of PSII and PSI combined with digitonin fractionation of thylakoid membranes indicated that UWO241 altered its thylakoid membrane architecture and reorganized the distribution of PSI and PSII units between granal and stromal lamellae. Although UWO241 grown at low salt and low temperature exhibited comparable thylakoid membrane appression to that of *C. reinhardtii* at its optimal growth condition, UWO241 grown under its natural condition of high salt resulted in swelling of the thylakoid lumen. This was associated with an upregulation of PSI cyclic electron flow by 50% compared to growth at low salt. Due to the unique 77K fluorescence emission spectra of intact UWO241 cells, deconvolution was necessary to detect enhancement in energy distribution between PSII and PSI, which was sensitive to the redox state of the plastoquinone pool and to the NaCl concentrations of the growth medium. We conclude that a reorganization of PSII and PSI in UWO241 results in a unique state transition phenomenon that is associated with altered protein phosphorylation and enhanced PSI cyclic electron flow. These data are discussed with respect to a possible PSII-PSI energy spillover mechanism that regulates photosystem energy partitioning and quenching.

Earth is a cold place, with 80% of its biosphere permanently below 5°C (Feller and Gerday, 2003; Margesin et al., 2007; Dolhi et al., 2013). Many of the algae that dominate these cold, aquatic habitats are psychrophiles, that is, obligately cold adapted (Morgan-Kiss et al., 2006; Dolhi et al., 2013; Siddiqui et al., 2013) and thrive in a variety of niches, from perennially ice-covered lakes to sea ice and snowfields (Vincent et al., 2004; Morgan-Kiss et al., 2006; Margesin et al., 2007; Lyon and Mock, 2014; Chrismas et al., 2015; Cvetkovska et al., 2017). Permanently frozen Antarctic lakes once assumed to be devoid of biodiversity have been shown to be teeming with diverse organisms adapted to life at the edge (Priscu et al., 1998; Bielewicz et al., 2011). These organisms are crucial components of one of the most sensitive ecosystems on Earth with respect to projected climate change scenarios (Vincent et al., 2004; Siddiqui et al., 2013; Kennicutt et al., 2014; Xavier et al., 2016). The Chlorophyta represent >33% of all confirmed photosynthetic psychrophiles, of which 23 species belong to the order Chlamydomonadales (Cvetkovska et al., 2017), which include some of the

[1]This work was supported by the Natural Sciences and Engineering Research Council of Canada (NSERC), with a Discovery Grant to N.P.A.H., a Postgraduate Fellowship to B.S.-M., and a Postdoctoral Fellowship to M.C., as well as individual contributions to D.R.S. and D.P.M., and by the Canada Foundation for Innovation and the Canada Research Chairs Program.

[2]These authors contributed equally to the article.

[3]Present Address: Department of Biology, University of Ottawa, Ottawa, Canada K1N 6N5.

[4]Author for contact: nhuner@uwo.ca.

[5]Senior author.

The author responsible for distribution of materials integral to the findings presented in this article in accordance with the policy described in the Instructions for Authors (www.plantphysiol.org) is: Norman P.A. Hüner (nhuner@uwo.ca).

B.S.-M., M.C., D.P.M., and N.P.A.H. conceived the study; B.S.-M., M.C., A.G.I., and M.P. performed the experiments; B. S.-M., M.C., D.R.S., A.G.I., and N.P.A.H. analyzed and interpreted the data; B, S.-M., M.C., A.G.I., and N.P.A.H. wrote the manuscript; all authors edited the manuscript.

www.plantphysiol.org/cgi/doi/10.1104/pp.19.00411

best-studied psychrophiles (Vincent et al., 2004; Morgan-Kiss et al., 2006; Margesin et al., 2007; Liu et al., 2011; Lyon and Mock, 2014; Chrismas et al., 2015; Cvetkovska et al., 2017). Recently, Mock et al. (2017) provided the first detailed analyses regarding the evolutionary genomics of the photosynthetic, cold-adapted diatom *Fragilariopsis cylindrus.*

Chlamydomonas sp. UWO241 was isolated from Lake Bonney, Antarctica, where it exists 17 m below the permanently ice-covered surface (Neale and Priscu, 1995; Priscu et al., 1998) at low but constant temperatures (4°C to 6°C) combined with high salt (HS) concentrations (700 mM; Lizotte and Priscu, 1994; Lizotte et al., 1996; Spigel and Priscu, 1996). Although the natural habitat of UWO241 is one of HS, its growth rate is maximal at low salt (LS; 10 mM) and low temperature (10°C; Morgan-Kiss et al., 2006) but dies at growth temperatures above 18°C, which classifies UWO241 as a halotolerant, obligate psychrophile (Lizotte and Priscu, 1992; Morgan et al., 1998; Morgan-Kiss et al., 2006; Pocock et al., 2007; Possmayer et al., 2011). In addition, UWO241 is found at the lake's lowest trophic zone, which is characterized by low photon flux density (<50 μmol photons m^{-2} s^{-1}) enriched in the blue-green region of the visible spectrum (450–550 nm) during the 6 months of austral summer. Nevertheless, maximal growth rates for UWO241 are attained at light levels (250 μmol photons m^{-2} s^{-1}) that are at least 5-fold higher than its natural growth light (Morgan-Kiss et al., 2006). Phylogenetic analyses of nuclear and chloroplast DNA sequences indicate that UWO241 represents a unique lineage within the Moewusinia clade of the Chlamydomonadales (Chlorophyceae, Chlorophyta) which is distantly related to the model green alga *Chlamydomonas reinhardtii* (Possmayer et al., 2016; Cvetkovska et al., 2019).

Structurally, UWO241 cells are present either as motile, biflagellate single cells or as immobile structures called palmelloids that are surrounded by a limiting membrane and comprised of up to 16 individual flagellated cells each containing a single chloroplast (Pocock et al., 2004; Possmayer et al., 2016). UWO241 exhibits the normal complement of photosynthetic pigments and an active xanthophyll cycle involved in nonphotochemical quenching (Morgan et al., 1998; Pocock et al., 2007; Szyszka et al., 2007). However, the thylakoids of UWO241 chloroplasts exhibit a PSI/PSII ratio of ~0.5, contributing to an unusually low chlorophyll a/b ratio (~1.8–2.2) for intact cells and isolated thylakoids (Morgan et al., 1998; Szyszka et al., 2007). In addition, Morgan et al. (1998) reported that UWO241 exhibits either an absence of or a reduction in 7 of the 11 Light harvesting complex 1a (Lhcas) normally present in *C. reinhardtii* (Bassi et al., 1992).

Adaptation of UWO241 to its extreme environment is associated with high levels of lipid unsaturation in the major chloroplast lipids monogalactosyldiacylglycerol, digalactosyldiacylglycerol, sulfoquinovosyldiacylglycerol, and phosphatidyldiacylglycerol, which result in a 30% higher unsaturation index coupled with a lower stability of the PSII supercomplex (SC) than is found in the mesophile, *C. reinhardtii*, upon exposure to high temperature stress (Morgan-Kiss et al., 2002a). The lipid and fatty acid composition for UWO241 are consistent with adaptation and acclimation of plants, algae, and cyanobacteria to low temperature (Wada et al., 1993; Nishida and Murata, 1996; Murata and Los, 1997; Moellering et al., 2010).

Functionally, UWO241 exhibits maximal light-saturated rates of photosynthesis near its optimal growth temperature of 8°C which are equivalent to maximal rates of photosynthesis in *C. reinhardtii* measured at its optimal growth temperature of 28°C (Pocock et al., 2007). Consequently, the light response curve for excitation pressure, measured as 1-qL, in UWO241 at its optimal growth temperature (8°C) is comparable to that of the closely related mesophile *Chlamydomonas raudensis* SAG49.72 at its optimal growth temperature of 28°C (Szyszka et al., 2007). Thus, UWO241 grown at 8°C maintains an energy balance comparable to that of SAG49.72 grown at 28°C, indicating that both the psychrophile and this mesophile maintain a comparable redox status of their intersystem photosynthetic electron transport chain in response to increasing photon flux density at their respective optimal growth temperatures. However, in contrast to other green algae, such as *Chlorella vulargis*, *Dunaliella salina*, and the cyanobacterium *Plectonema boryanum*, UWO241 does not exhibit any major changes in pigmentation, Chl a/b ratio, or level of light-harvesting complex II (LHCII) polypeptides in response to growth at high light (Morgan-Kiss et al., 2006). One of the most unusual features of UWO241 is its apparent inability to undergo a typical modulation of energy distribution between PSII and PSI measured by changes in 77K fluorescence emission spectra in response to either elevated temperature or the absence of O_2, conditions which typically induce state transitions in green algae (Morgan-Kiss et al., 2002a, 2002b; Takizawa et al., 2009; Ünlü et al., 2014). However, UWO241 exhibits an unusual 77K fluorescence emission spectrum in which the expected PSI emission band normally evident at 712 nm in *C. reinhardtii* is absent in this psychrophile (Morgan-Kiss et al., 2002b; Szyszka et al., 2007; Takizawa et al., 2009; Szyszka-Mroz et al., 2015; Cook et al., 2019). This phenomenon was coupled with the inability to detect LHCII phosphorylation in UWO241 using phospho-Thr (P-Thr) antibodies (Morgan-Kiss et al., 2002b; Takizawa et al., 2009). Based on these data, it was concluded that UWO241 is deficient in state transitions (Morgan-Kiss et al., 2002a).

UWO241 exhibits a cytochrome b_6f complex ($Cytb_6/f$) composed of a Cyt*f* subunit that is 7 kD smaller than that of *C. reinhardtii* (Morgan et al., 1998; Morgan-Kiss et al., 2002a, 2006; Gudynaite-Savitch et al., 2006; Szyszka et al., 2007). Transformation of *C. reinhardtii* with *petA* from UWO241 demonstrated that the 7 kD smaller Cyt*f* does not account for the apparent inability of UWO241 to undergo state transitions (Gudynaite-Savitch et al., 2006). Consequently, in addition to

being a halotolerant psychrophile (Takizawa et al., 2009), UWO241 appears to exhibit an aberrant capacity to regulate energy distribution between PSII and PSI through traditional state transitions, as assessed by 77K fluorescence emission spectra and LHCII phosphorylation based on immunodetection of P-Thr residues, while maintaining high rates of photosynthesis under its normal growth regime. This is unique for known green algae and terrestrial plants (Nelson and Ben-Shem, 2004; Eberhard et al., 2008; Rochaix, 2011, 2014). However, UWO241 has retained the capacity for long-term adjustment of energy distribution between PSI and PSII by modulating photosystem stoichiometry in response to light quality (Morgan-Kiss et al., 2005), and it normally maintains high rates of PSI cyclic electron flow (CEF) via a novel PSI SC whose stability appears to be dependent on its phosphorylation status as well as the Fe concentrations in the growth medium (Szyszka-Mroz et al., 2015; Cook et al., 2019).

The extreme environment in which UWO241 has evolved not only includes constant low temperature combined with constant HS (700 mM), but also minimal short-term fluctuations in the low light conditions during the austral summer coupled with complete darkness during the austral winter (Morgan-Kiss et al., 2006). Thus, it would appear that adaptation to such a constant environment would minimize the necessity of state transitions, which was initially supported by the lack of LHCII phosphorylation as measured by P-Thr antibody immunodetection combined with minimal modulation of PSI/PSII energy distribution based on 77K emission spectroscopy of cells exposed to aerobic versus anaerobic conditions (Morgan-Kiss et al., 2002b; Takizawa et al., 2009). However, recent examination of the UWO241 genome (Cvetkovska et al., 2018) indicated the presence of thylakoid protein kinases *Stt7* and *Stl1*. Thus, the goal of the present research was to address the following questions: (1) Are *Stt7* and *Stl1* expressed and active in UWO241? (2) If so, does UWO241 perform redox-dependent state transitions despite its novel 77K fluorescence emission spectra? (3) Are the novel 77K fluorescence emission spectra a consequence of an altered organization of PSI and PSII in thylakoids of UWO241? We address these questions through a molecular, biochemical, and biophysical comparison of the photosynthetic apparatus of the psychrophile *Chlamydomonas* sp. UWO241 with the model mesophilic green alga *C. reinhardtii*.

RESULTS

Radiolabeling with [γ-^{33}P]ATP

To assess the validity of our previous assumption that the absence of LHCII phosphorylation based on immunodetection with P-Thr antibodies coupled with the apparent inability to detect modulation of PSII/PSI energy distribution by 77K fluorescence emission indicates that UWO241 is deficient in state transitions (Morgan-Kiss et al., 2002b; Szyszka et al., 2007; Takizawa et al., 2009), we examined the extent of thylakoid polypeptide phosphorylation directly using radiolabeling with ^{33}P, the most sensitive and most direct technique for the detection of phosphoproteins (Aro et al., 2004; Vener, 2008). Suc gradient purified thylakoid membranes of *C. reinhardtii* and UWO241 were radiolabeled in vitro in the presence of [γ-^{33}P]ATP at the optimal growth temperatures for each species, 23°C and 8°C, respectively, following 15 and 30 min of light exposure (Fig. 1A). Radiolabeling with [γ-^{33}P]ATP revealed that the major sites of thylakoid protein phosphorylation in UWO241 as well as in *C. reinhardtii* 1690 were the major LHCII polypeptides (Fig. 1A). Staining with ProQ Diamond also indicated that LHCII was indeed the major site of thylakoid protein phosphorylation, although labeling with [γ-^{33}P]ATP appeared to be quantitatively and qualitatively more sensitive than staining with ProQ Diamond (Supplemental Fig. S1). In contrast to *C. reinhardtii*, UWO241 exhibited minimal labeling of the minor LHCII components p9 and p10 (Light harvesting complex b4 [Lhcb4] and Lhcb5) and the PSII core polypeptides CP43 and D2 (Fig. 1, A and B). The identity of these radiolabeled PSII thylakoid polypeptides was validated by immunoblotting (Fig. 1B). In addition, UWO241 exhibited a ^{33}P-labeled, high-molecular mass polypeptide (130 kD) as well as a 17 kD polypeptide, neither of which was detected in *C. reinhardtii* by radiolabeling (Fig. 1A, arrows). Thus, UWO241 thylakoid protein kinases appear to be active in the phosphorylation of the major LHCII thylakoid polypeptides, which is consistent with UWO241 having levels of Stt7 comparable to those of the mesophiles *C. reinhardtii* 1690 and SAG49.72 (Fig. 1C). However, the thylakoid polypeptide phosphorylation pattern for UWO241 was distinct from that of *C. reinhardtii* regardless of the method of detection (Fig. 1, A and B; Supplemental Fig. S1).

Light, Temperature, and Salt Dependence of LHCII Phosphorylation

The light dependence for thylakoid protein phosphorylation in *C. reinhardtii* and UWO241 was examined at their optimal growth temperatures (Fig. 2A). As expected, levels of [γ-^{33}P]ATP incorporation were highest during illumination for both minor (36–38 kD) and major (25–31 kD) LHCII bands of *C. reinhardtii*, decreased in the dark (Fig. 2A), and were sensitive to the protein kinase inhibitor staurosporine (Supplemental Fig. S2). UWO241 also exhibited light-dependent phosphorylation of pA/B + D1 as well as pC polypeptides (Fig. 2A). Thus, consistent with expectations, thylakoid protein kinase activity in UWO241 is light dependent but appears to be insensitive to staurosporine compared to that of *C. reinhardtii* (Fig. 2A; Supplemental Fig. S2).

Since the optimal growth temperatures for *C. reinhardtii* and UWO241 differ markedly, we examined the

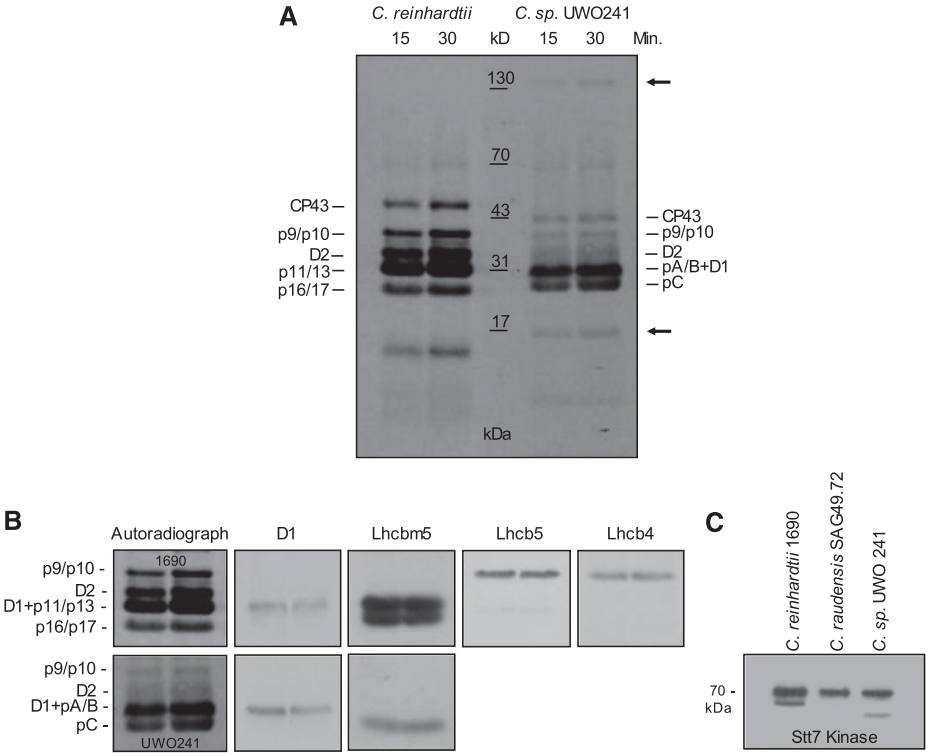

Figure 1. An autoradiograph is shown of [ɣ-33P]ATP-labeled thylakoid proteins in *C. reinhardtii* 1690 and *Clamydomonas* sp. UWO241 grown at their optimal growth temperatures at 8°C and 23°C in *Chlamydomonas* sp. UWO241 and *C. reinhardtii* respectively, following 15 and 30 min of light exposure (A). B, [ɣ-33P]ATP-labeled phosphoprotein bands in *C. reinhardtii* 1690 (top) and *Clamydomonas sp.* UWO241 (bottom) are identified using immunoblotting with antibodies specific for D1, Lhcbm5, Lhcb5, and Lhcb4. The position of the D2 protein was assigned based on a previous study (Lemeille et al., 2010). C, *C. reinhardtii* 1690, *C. raudensis* SAG49.72, and *Clamydomonas* sp. UWO241 thylakoid membranes are immunoblot analyzed by probing with antibodies specific for the Stt7 kinase.

effects of incubation temperature on the thylakoid polypeptide phosphorylation profiles (Fig. 2B). As expected, the extent of thylakoid polypeptide phosphorylation was greater at 23°C than at 8°C for the mesophile *C. reinhardtii* (Fig. 2B). In contrast, the extent of thylakoid polypeptide phosphorylation for UWO241 was higher upon incubation at its optimal growth temperature of 8°C than at 23°C (Fig. 2B), which is a nonpermissive growth temperature for UWO241 (Morgan-Kiss et al., 2006; Possmayer et al., 2011). However, growth of UWO241 under either HS or LS appeared to have minimal effects on the level of LHCII phosphorylation as assessed by ProQ Diamond staining (Supplemental Fig. S1).

Putative Structures of the Stt7 and Stl1 Thylakoid Protein Kinases

The data presented in Figures 1 and 2 and Supplemental Figure S1 confirm that UWO241 exhibits active thylakoid protein kinases. However, based on the temperature dependence of our [γ-^{33}P]ATP labeling studies and the apparent decreased sensitivity to the kinase inhibitor, staurosporine, we hypothesized that the UWO241 thylakoid protein kinases may be structurally and functionally distinct and adapted to function at low temperatures. Screening of the UWO241 genome and transcriptome revealed that, as with *C. reinhardtii*, Stt7 was encoded by a single gene in UWO241 with an average 91× coverage per nucleotide at the transcriptome level. The nucleotide sequence for *Stt7* from UWO241 encoded a 663 amino acid protein, in contrast to 754 amino acids in *C. reinhardtii* (Fig. 3). Furthermore, UWO241 Stt7 shared 42% sequence identity with its orthologs from *C. reinhardtii* and *Volvox carteri* and 44% identity with Stt7 from the cold-adapted alga *Coccomyxa subellipsoidea* (Fig. 3). However, the sequences had a very low identity in the N- and C-terminals of the protein while the protein kinase domain had a higher level of identity among species (61% with *C. reinhardtii*, 62% with *V. carteri*, and 59% with *C. subellipsoidea*; Fig. 3).

Several common features were identified in the sequences of Stt7 kinase from *C. reinhardtii* and UWO241 (Figs. 3 and 4, A and B). First, the lumen exposed N terminus contained two highly conserved Cys residues, which are important for the regulation of Stt7 kinase (Lemeille et al., 2009; Wunder et al., 2013; Shapiguzov et al., 2016). These residues (Cys-68 and Cys-73) were conserved among all species examined including UWO241. Similarly, several key residues involved in ATP binding have been identified in the protein kinase domain (Lys-172, Glu-181, Asp-288, and Asn-293; De Bondt et al., 1993; Guo et al., 2013) and are conserved among all species examined here. Another functionally important domain is the activation loop, which may adopt variable conformations and thus regulate protein kinase activity (Nolen et al., 2004). This region, including the highly conserved Asp-307 residue, is very similar among the species examined.

Comparing the predicted structures of the kinase domains of the Stt7 kinase from UWO241 and that from *C. reinhardtii* also revealed several differences in the

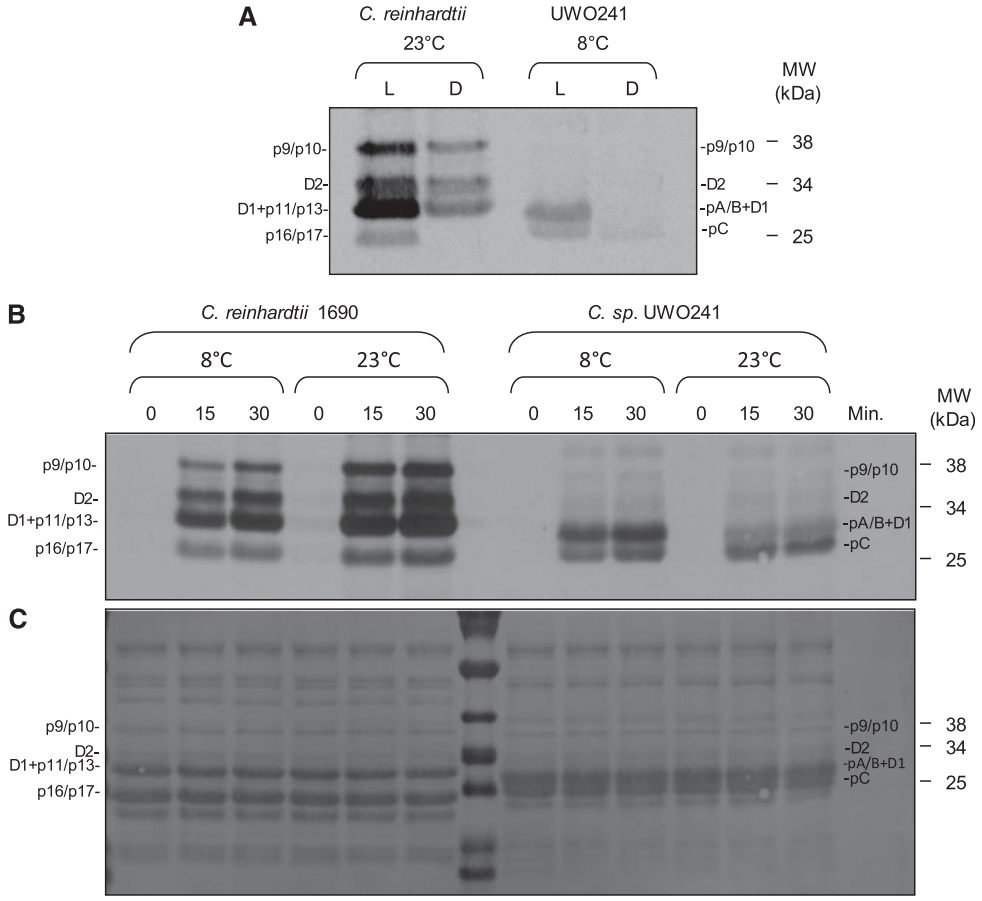

Figure 2. In vitro [γ-^{33}P]ATP labeling of LHCII proteins is shown in *C. reinhardtii* and *Clamydomonas* sp. UWO241. A, Levels of thylakoid membrane phosphorylation after 15 min of exposure to light (L) were compared to those following 15 min of darkness (D) at 8°C and 23°C in both *C. reinhardtii* and *Clamydomonas* sp. UWO241. B, Purified thylakoids were phosphorylated at 8°C and 23°C for 0, 15, and 30 min, in the presence of light (200 μmol m^{-2} s^{-1}). C, The [γ-33P]ATP-labeled nitrocellulose membrane was stained with Ponceau S to visualize abundance of LHCII.

predicted tertiary structure of the Stt7 kinases in UWO241 and *C. reinhardtii* at the level of the kinase domain (Fig. 4, A and B; Supplemental Fig. S3, A and B). First, in a highly conserved Gly-rich region (P-loop) with a LGxGxxGxV motif involved in binding of ATP, substrate recognition, catalysis, and kinase activity regulation (Bossemeyer, 1994; Hanks and Hunter, 1995), a conserved Gly is substituted by Ala at position 147 in both cold-adapted species, UWO241 and *C. subellipsoidea* (Fig. 4). Second, a hairpin motif containing a $PX_{7/8}LW$ has been identified adjacent to the activation loop, which is characteristic for the Stt7/STN7 family of thylakoid protein kinases and is essential for the maintenance of protein stability and activity (Guo et al., 2013). In UWO241, the highly conserved Pro residue is substituted by Ala at position 350. Furthermore, this region also exhibits substantial conformational differences in the predicted tertiary structures between Stt7 from UWO241 and that from *C. reinhardtii* (Fig. 4, A and B; Supplemental Fig. S3A). Last, a putative autophosphorylation domain was identified in *C. reinhardtii* (DAGLASMEEAILK; Lemeille et al., 2010; Lemeille and Rochaix, 2010) which is completely absent from UWO241, including the phosphorylation site of Ser at position 503 (Figs. 3 and 4, A and B; Supplemental Fig. S3, A and B). Our analyses indicated that the autophosphorylation domain in the predicted structure of Stt7 from *C. reinhardtii* was part of an α-helix, whereas this domain was not detected in the corresponding regions of Stt7 from UWO241 (Supplemental Fig. S3, A and B).

Screening of the UWO241 genome and transcriptome also revealed that in contrast to *C. reinhardtii* and the other algal species examined, UWO241 encoded two homologs of Stl1, Stl1-A and Stl1-B (Fig. 5), at both the genome and transcriptome levels. Both *Stl1* transcripts (*Stl1-A* and *Stl1-B*) from UWO241 were represented by a similar number of reads in the transcriptome (average coverage per nucleotide = 125× and 115×, respectively), indicating that both genes were expressed at similar levels in UWO241.

The nucleotide-derived protein sequences from UWO241 encoded proteins of 483 amino acids (Stl1-A) and 581 amino acids (Stl1-B). These proteins shared a sequence identity of 55% with each other, 52% with the protein from *C. reinhardtii*, 51% with the protein from *V. carteri*, and 48% with the protein from *C. subellipsoidea* (Fig. 5). Similar to Stt7, the Stl1 kinase domain shared the highest sequence similarity between species (63% between Stl1-A and Stl1-B, 62% with *C. reinhardtii*, 61% with *V. carteri*, and 56% with *C. subellipsoidea*). These differences in sequence were reflected in the predicted tertiary structure of Stl1-A and Stl1-B from UWO241 when compared to their mesophilic counterpart

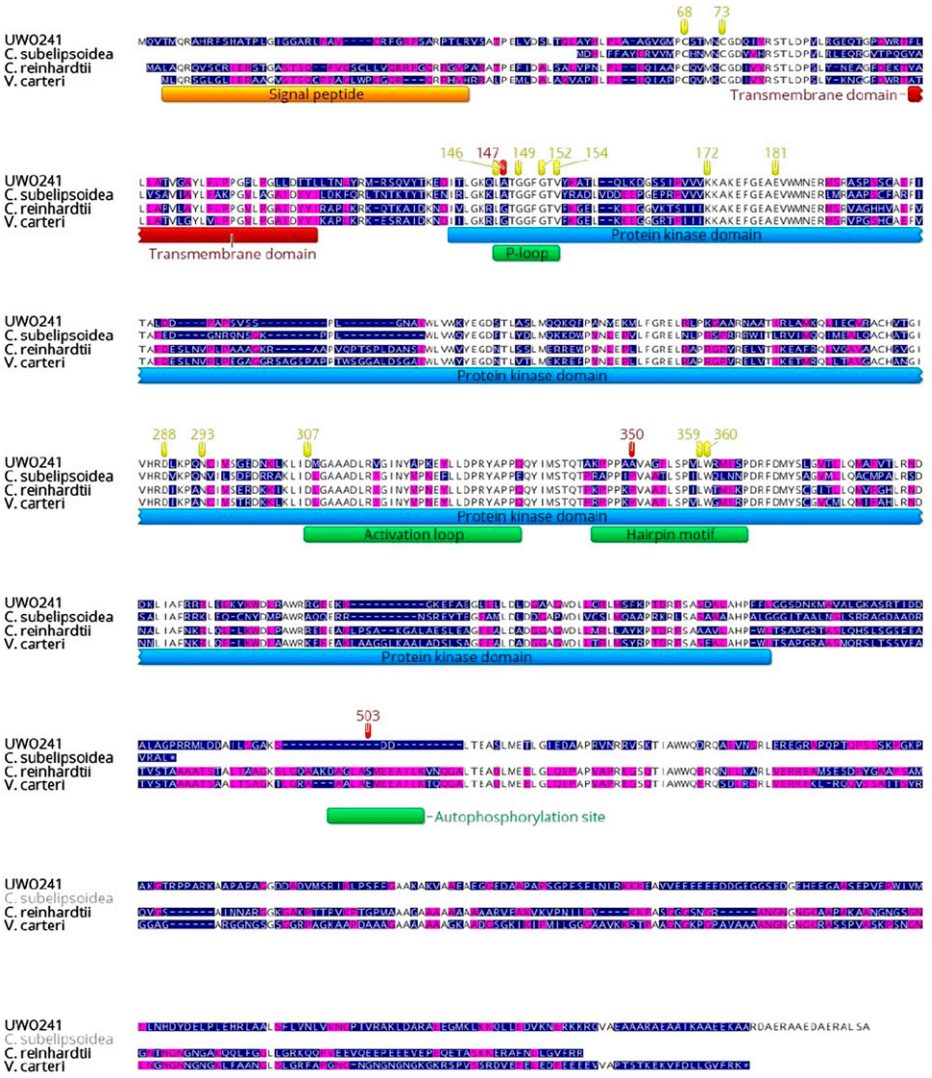

Figure 3. The Stt7 protein of *Chlamydomonas* sp. UWO241 is aligned with those of *C. subellipsoidea*, *C. reinhardtii*, and *V. carteri*. The color of the residue depends on the level of conservation among species (white, fully conserved; yellow, 80–100% similar; purple, 60–80% similar; blue, <60% similar). Regions corresponding to the putative signal peptide, transmembrane domain, and kinase domain are indicated. The positions of important sequence patterns are marked with a green box, and highly conserved residues are highlighted in yellow (according to Guo et al. [2013] and Lemeille et al. [2010]).

from *C. reinhardtii* (Supplemental Fig. S4, A–C). For instance, the major differences were localized to the less-conserved N terminus of the protein, while the more conserved domain retained the typical protein kinase tertiary structure. Recently, a Stt7-dependent phosphorylation pattern was identified in the sequence of Stl1 from *C. reinhardtii* (LQADDQGVTQRS; Lemeille and Rochaix, 2010). The phosphorylation site, Thr-167, was conserved in the Stl1 sequences of *C. reinhardtii* and *V. carteri*, but it was absent from both the psychrophile UWO241 and the cold-adapted *C. subellipsoidea* (Fig. 5).

We confirmed the presence of genes encoding *Stt7* and *Stl1* in the UWO241 genome and annotated the exons and introns (Supplemental Fig. S5). In all cases, the UWO241 genes had a longer nucleotide sequence when compared to *C. reinhardtii* and the noncoding, intronic regions constituted a greater percentage of the full gene length (Supplemental Table S1). Furthermore, we suggest that *Stl1*, unlike *Stt7*, may have undergone a recent duplication event in UWO241.

Regulation of PSII/PSI Energy Distribution

Is energy distribution between PSII and PSI in UWO241 dependent upon the redox state of the plastoquinone pool? This was assessed and quantified by modulating the redox state of the plastoquinone pool in the presence of the photosynthetic electron transport inhibitors 3-(3,4-dichlorophenyl)-1,1-dimethylurea (DCMU) and 2,5-dibromo-6-isopropyl-3-methyl-1,4-benzoquinone (DBMIB; Fork and Satoh, 1986; Papageorgiou and Govindjee, 2011). Irrespective of the conditions under which the 77K fluorescence emission spectra were collected, those of UWO241 were distinct from those of *C. reinhardtii* 1690 with respect to the absence of a prominent emission peak at 711 nm that is typical for PSI in *C. reinhardtii* (Fig. 6; Table 1). *C. reinhardtii* exhibited the typical state 1 (+DCMU; Fig. 6A)-to-state 2 (+DBMIB; Fig. 6C) transition observed by 77K fluorescence spectroscopy. As expected, deconvoluted spectra for *C. reinhardtii* indicated a 2.21-fold increase in the PSII/PSI ratio (Table 1). Although the

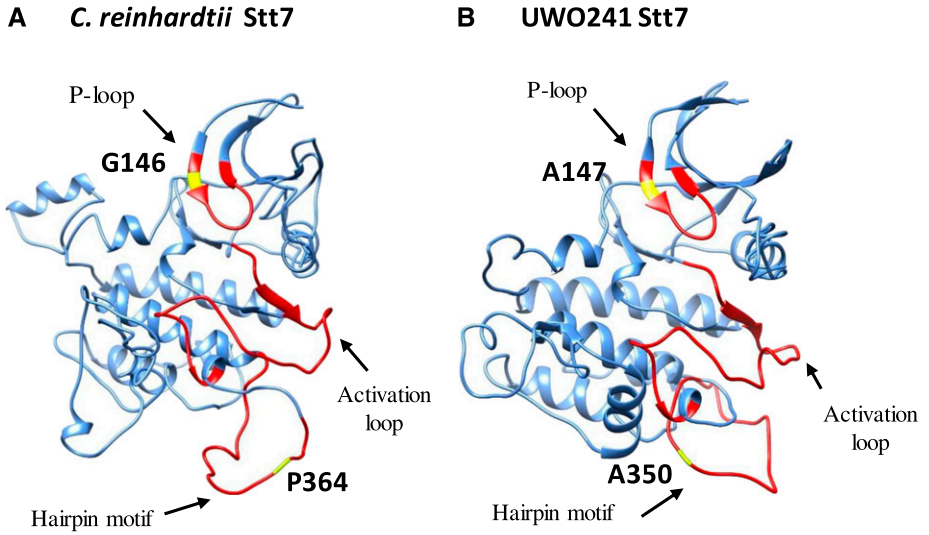

Figure 4. Predicted secondary structures of Stt7 kinase domains in *C. reinhardtii* (A) and UWO241 (B). The important domains in each case are shown in red and highlighted with a black arrow (according to Guo et al. [2013] and Lemeille et al. [2010]). The critical residues that differ between *C. reinhardtii* and UWO241 are shown in yellow and labeled.

PSII/PSI ratio in nontreated UWO241 control cells was approximately double that in *C. reinhardtii* (Table 1), the effects of DCMU and DBMIB on the fluorescence emission spectra of UWO241 appeared to be qualitatively novel (Fig. 6, B and D) compared to their effects on those of *C. reinhardtii*. Even in the presence of either DCMU (Fig. 6B) or DBMIB (Fig. 6D), no distinct PSI 77K fluorescence emission band at 712 nm was evident, consistent with previous results (Morgan-Kiss et al., 2002a; Szyszka et al., 2007; Takizawa K et al., 2009; Szyszka-Mroz et al., 2015; Cook et al., 2019). Nevertheless, deconvolution of the 77K emission spectra (DCMU versus DBMIB) for UWO241 indicated that the psychrophile exhibited a change in its PSII/PSI ratio (2.39; Table 1) comparable to that of *C. reinhardtii* due to a relative modulation of the putative PSI emission band at 706 nm (Fig. 6, B and D).

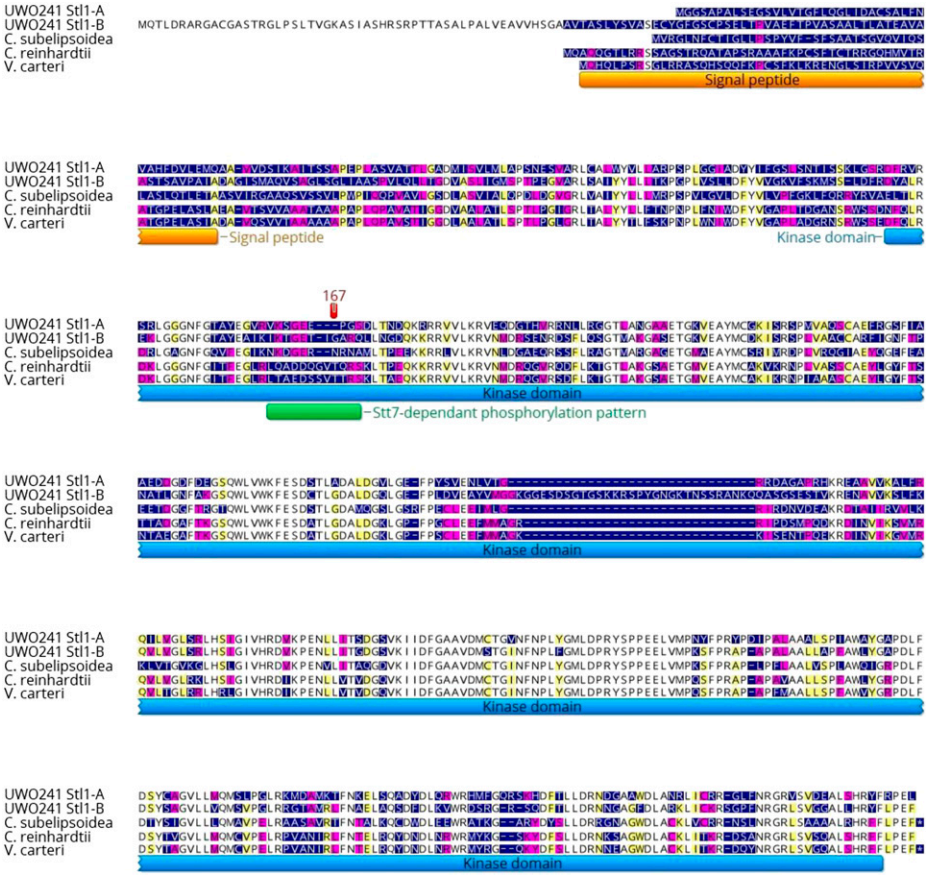

Figure 5. Stl1 proteins of *Chlamydomonas* sp. UWO241 are aligned with those of *C. subellipsoidea*, *C. reinhardtii*, and *V. carteri*. The color of the residue depends on the level of conservation among species (white, fully conserved; yellow, 80–100% similar; purple, 60–80% similar; blue, <60% similar). Regions corresponding to the putative signal peptide and kinase domain are indicated. The position of a putative Stt7-dependent phosphorylation pattern is marked with a green box, and Threonine167, the position of a Stt7-dependent phosphorylation site in *C. reinhardtii* (Lemeille et al., 2010), is highlighted in red. Both Stl1 isoforms from UWO241 lack this phosphorylation pattern.

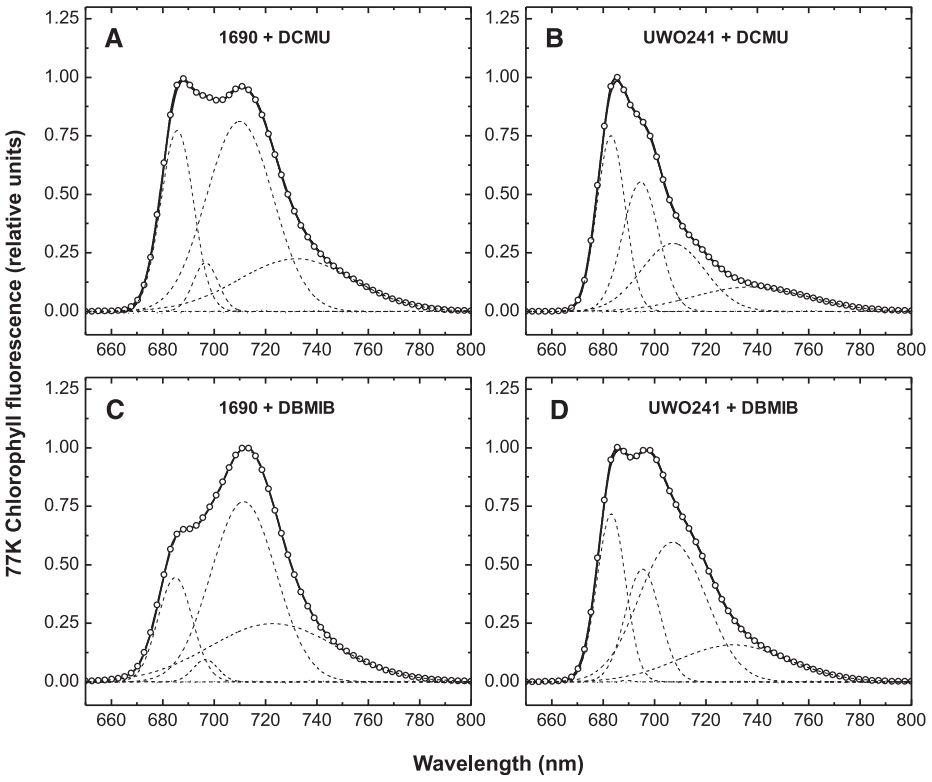

Figure 6. Gaussian deconvolution of fluorescence emission spectra at 77K was performed on *C. reinhardtii* 1690 and *Clamydomonas* sp. UWO241 cell cultures treated with inhibitors. The effects of DCMU (A and B) and DBMIB (C and D) on 77K emission spectra in *C. reinhardtii* 1690 (A and C) and *Clamydomonas sp.* UWO241 (B and D) are shown. Cell cultures were incubated for 5 min in the dark in the presence of either 5 μM DCMU or 3 μM DBMIB, followed by a 5 min exposure to growth irradiance. Chl fluorescence was excited at 436 nm.

Although PSI is present in UWO241 (Szyszka-Mroz et al., 2015), deconvolution of the 77K emission spectra of UWO241 was required to detect a putative PSI emission band blue-shifted to 706 nm (Table 1).

Since the natural environment of UWO241 is one of HS (700 mM NaCl), we assessed the effects of salt concentration on the in vivo energy distribution between PSII and PSI (Fig. 7) in cells grown at either HS (700 mM) or LS (70 mM). Although exposure to darkness versus light (Fig. 7) had minimal effects on the quality of the UWO241 emission spectra, growth of UWO241 under HS quantitatively favored PSII

Table 1. *Gaussian Parameters for the Subband Decomposition of Low Temperature (77K) Chlorophyll Fluorescence Emission Spectra of Two* Chlamydomonas *Strains (1690 and UWO241)*

C. reinhardtii and *C lamydomonas* sp. UWO241 were grown under their respective optimal growth temperatures in either the absence (control) or presence of DCMU and DBMIB. The percentage areas of the spectral forms have been calculated from the total area given by the sum of all bands. The FWHM of each band is the sum of the left and right half width at half maximum values. PSII/PSI represents the ratio between the areas of PSII related peaks (λ1, λ2, and λ3) and the area of the PSI peak (λ4).

Parameters	1690			UWO241		
	Control	+ DCMU	+ DBMIB	Control	+ DCMU	+ DBMIB
1 λ max	683.4	683.2	673.7	–	–	683.1
FWHM	10.89	8.56	2.00	–	–	10.65
Area %	18.24	9.54	0.02	–	–	21.60
2 λ max	685.9	685.6	684.9	683.9	683.0	689.2
FWHM	5.18	12.32	13.01	10.26	10.53	3.08
Area %	3.87	20.71	15.40	28.43	29.53	0.06
3 λ max	693.3	696.7	696.6	695.5	694.6	695.3
FWHM	10.85	9.19	9.10	12.45	13.71	13.17
Area %	10.23	4.22	2.35	21.86	27.95	17.74
4 λ max	710.5	709.9	711.4	705.9	707.1	707.0
FWHM	23.83	25.63	25.14	26.84	24.54	25.81
Area %	43.38	44.38	50.51	33.91	25.82	42.36
5 λ max	728.7	731.8	722.9	739.7	737.3	730.5
FWHM	47.26	44.50	49.0	42.44	43.96	42.28
Area %	24.27	21.16	31.69	15.73	16.59	18.22
PSII/PSI	0.745	0.776	0.351	1.480	2.229	0.930

emission relative to PSI emission based on deconvolution (Table 2). However, the PSI quantum yield (0.054 ± 0.001) of UWO241 grown under HS was almost double that observed under LS for either UWO241 (0.027 ± 0.002) or *C. reinhardtii* (0.029 ± 0.001; Supplemental Fig. S6; Table 3). Thus, the in vivo energy distribution observed between PSII and PSI, as well as the rates of PSI CEF, measured as $t_{1/2}$ of $P700^+$ decay (Table 3), are dependent upon the salt concentration in the growth medium of the halotolerant psychrophile UWO241. Under HS, the estimated PSI cross section (σ), as well as the estimated rate of CEF ($t_{1/2}$), for UWO241 was double that observed upon growth under LS. The latter was comparable to that observed for *C. reinhardtii* grown under standard conditions (Table 3).

Mg^{2+} concentration has been shown to affect thylakoid membrane stacking, thylakoid lateral heterogeneity, and state transitions (Bonaventura and Myers, 1969; Murata, 1969; Wollman and Diner, 1980; Barber, 1982; Papageorgiou and Govindjee, 2011). The results of Figure 8 illustrate the effects of increasing $MgCl_2$ concentration on energy distribution between PSII and PSI in UWO241 (black symbols) and *C. reinhardtii* (white symbols). As expected, increasing the $[Mg^{2+}]$ favored a shift in the relative emission from PSI to PSII (Fig. 8) in both the psychrophile and *C. reinhardtii*.

Thus, contrary to our previous conclusions (Morgan-Kiss et al., 2002b), UWO241 does indeed undergo state transitions that are dependent upon the redox state of the intersystem electron transport chain (Fig. 6). However, the state transition phenomenon as measured by 77K fluorescence in UWO241 appears to be more sensitive to NaCl concentration of the growth medium than to exposure to either light or darkness (Fig. 7; Table 2). Furthermore, this is associated not only with lower levels of LHCII phosphorylation but with a distinct thylakoid protein phosphorylation pattern compared to that of *C. reinhardtii* (Figs. 1 and 2; Supplemental Fig. S1).

Organization of the UWO241 Photosynthetic Apparatus

Based on the results presented above, we hypothesized that the distinct 77K fluorescence emission spectra observed during state transitions of UWO241compared to *C. reinhardtii* cells may be explained, in part, by a difference in the relative organization of the photosynthetic apparatus due to the adaptation of UWO241 to its extreme environment characterized by low temperature and HS.

Pigment-protein complexes from *C. reinhardtii* and UWO241 were purified by Suc density gradient centrifugation which generated four major Chl-containing complexes (Fig. 9A). SDS-PAGE (Fig. 9, B and C) and 77K fluorescence emission (Fig. 9, H and I) confirmed

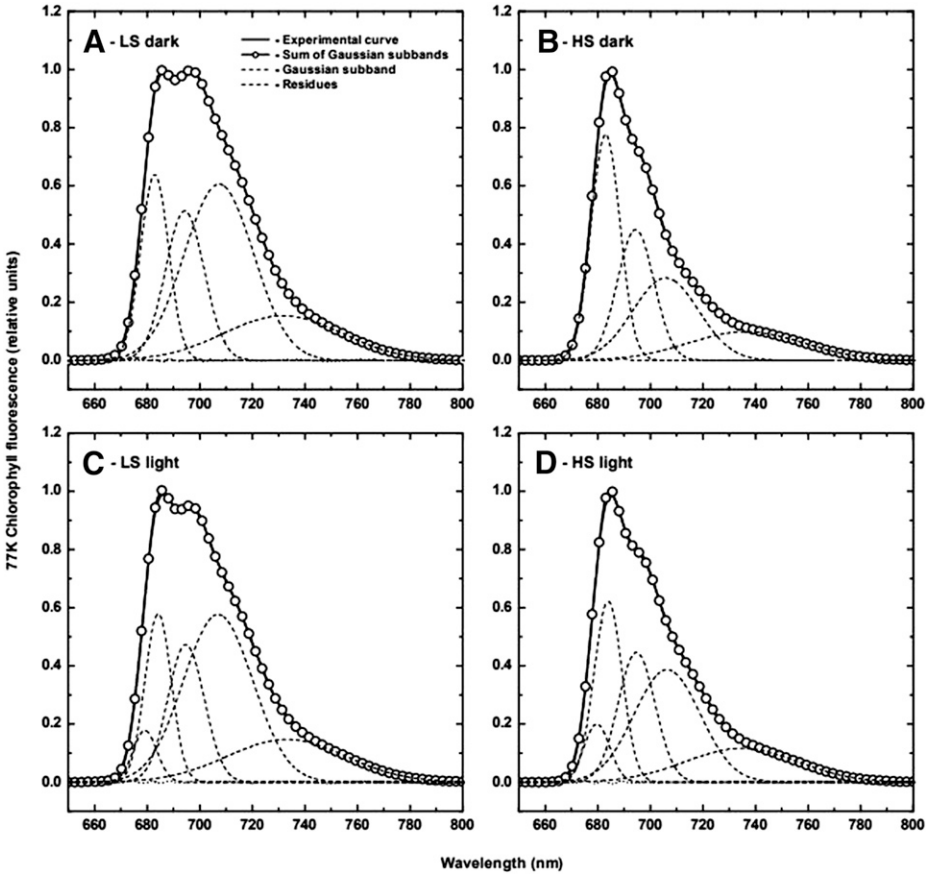

Figure 7. Gaussian deconvolution of fluorescence emission spectra at 77K was performed on *Clamydomonas sp* UWO241 cell cultures grown in BBM, supplemented with either LS (70 mM NaCl; A and C) or HS (700 mM; B and D). Cultures were exposed to either dark (A and B) or light (C and D) for 15 min, prior to freezing with liquid nitrogen.

Table 2. *Gaussian Parameters for the Subband Decomposition of Low-Temperature (77K) Chlorophyll Fluorescence Emission Spectra of* Clamydomonas *sp. UWO241 Grown in LSand HS Media and Exposed to Light and Dark Treatments*

The percentage areas of the spectral forms have been calculated from the total area given by the sum of all bands. The FWHM of each band is the sum of the left and right HWHM values. PSII/PSI represents the ratio between the areas of PSII-related peaks (λ1, λ2, and λ3) and the area of the PSI peak (λ4). Mean values ± SE were calculated from six to nine measurements in three to four independent experiments.

Parameters	LS		HS	
	Dark	Light	Dark	Light
1 λ max	675.5	679.2	682.9	679.7
FWHM	3.96	8.50	10.59	9.32
Area %	0.10	4.44	32.90	7.19
2 λ max	682.8	684.2	689.1	683.9
FWHM	10.15	9.55	3.02	10.24
Area %	18.12	9.49	0.06	24.46
3 λ max	694.3	694.8	694.4	694.7
FWHM	14.43	13.59	13.57	13.70
Area %	20.38	18.43	23.87	23.20
4 λ max	707.3	707.0	705.8	706.4
FWHM	26.09	26.12	24.76	24.86
Area %	42.82	42.42	26.98	35.76
5 λ max	731.6	732.9	736.4	734.6
FWHM	44.85	44.95	43.58	42.50
Area %	18.55	18.49	16.46	18.27
PSII/PSI	0.90	0.76	2.10	1.53

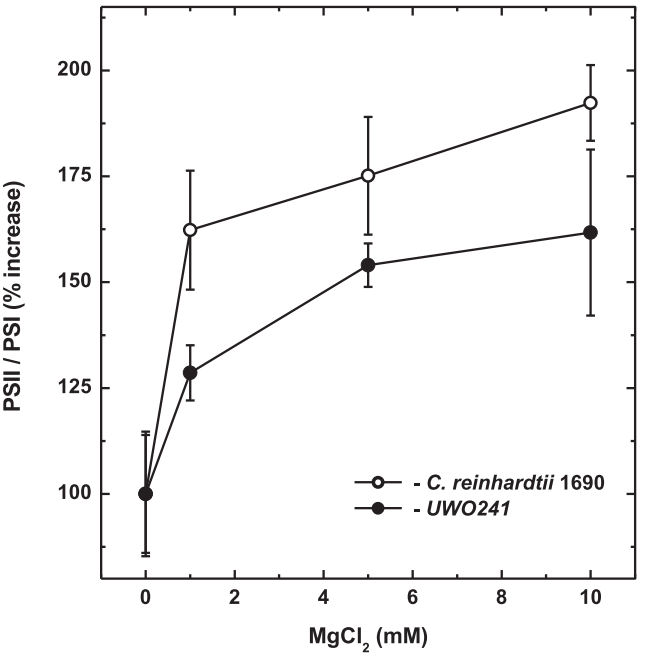

Figure 8. The effect of $MgCl_2$ concentration on the PSII/PSI ratio in thylakoid membranes of *C. reinhardtii* and *Clamydomonas* sp. UWO241 is shown. Thylakoid membranes were isolated in buffer (0.3 M sorbitol and 50 mM tricine, pH 7.8), containing varying concentrations of $MgCl_2$: 0, 1, 5, and 10 mM. Membranes were treated in the dark at 5°C and immediately frozen in liquid nitrogen. The PSII/PSI ratio is represented by the ratio between the areas of PSII related peaks (λ1, λ2, λ3) and the area of the PSI peak (λ4), as calculated from 77K chlorophyll fluorescence traces. All data represent the means of three individual experiments.

the identity of each band as illustrated in Figrue 9A. Although neither intact cells (Fig. 6) nor isolated thylakoids of UWO241 (Fig. 9G) exhibited a distinct and prominent emission band associated with PSI at 712 nm, Suc density-purified PSI from UWO241 thylakoids did exhibit the predicted PSI emission band at 712 nm (Fig. 9I), similar to that observed for *C. reinhardtii* (Fig. 9H).

Although the polypeptide complement of the four purified chlorophyll-protein complexes varied between the two species (Fig. 9, B and C), P-Thr antibodies detected strong phosphorylation of LHCII in *C. reinhardtii* (Fig. 9D) but failed to detect any apparent LHCII phosphorylation in UWO241 (Fig. 9E). Instead, the apparent phosphorylation sites in UWO241 detected using P-Thr antibodies were associated with a high molecular mass (>130 kD) and a 17 kD polypeptide of the PSI-Cyt b_6/f SC (Fig. 9E), as reported previously (Szyszka-Mroz et al., 2015), in addition to the PSII core polypeptides (Fig. 9E). Although the detection of LHCII polypeptide phosphorylation by P-Thr antibodies and ProQ Diamond staining were consistent with ^{33}P-labeling in *C. reinhardtii*, comparison of phosphorylation profiles of LHCII by either ^{33}P-labeling (Figs. 1 and 2) or staining with ProQ Diamond (Supplemental Fig. S1) were incongruent with the detection of LHCII polypeptide phosphorylation by P-Thr antibodies in UWO241. Thus, it appears that the LHCII phosphorylation sites in UWO241 were poorly recognized by P-Thr antibodies.

The organization of the thylakoid membrane was further investigated through an examination of the membrane distribution of the major thylakoid protein complexes ($Cytb_6/f$, PSI, PSII, and LHCII) by digitonin fractionation into granal, margin, and stromal fractions of UWO241 and *C. reinhardtii* (Fig. 10; Supplemental Fig. S7). As expected, the $Cytb_6/f$ complex (Cyt*f*) and

Table 3. *Effects of Growth Temperature and Growth Medium on the Effective PSI Absorbance Cross Sections (σ) and P700+ decay ($t_{1/2}$) of* C. reinhardtii *and* Chlamydomonas *sp. UWO241 Intact Cells*

VARIANTS	PSI Cross Section		$t_{1/2}^{P700+\ decay}$	
	σ	%	(s)	%
C. reinhardtii (28°C)	0.02909 ± 0.0005	100.0 ± 0.2	0.207 ± 0.017	100 ± 8.2
UWO241 (5°C, HS)	0.05375 ± 0.0006	184.8 ± 1.1	0.093 ± 0.007	44.9 ± 3.4
UWO241 (5°C, LS)	0.02696 ± 0.0022	92.7 ± 8.2	0.206 ± 0.013	99.5 ± 6.3

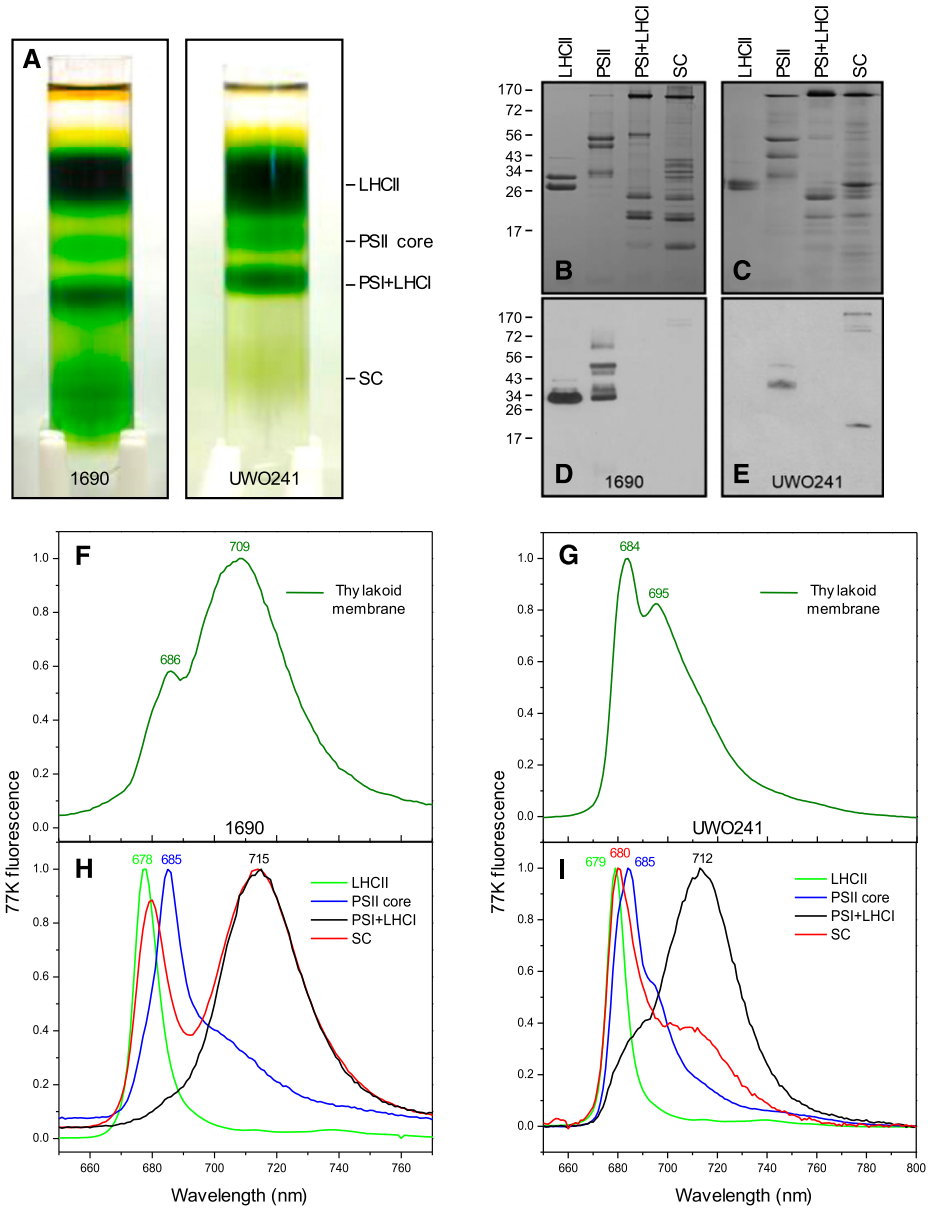

Figure 9. A, Thylakoid membrane complexes in *C. reinhardtii* 1690 and *Clamydomonas* sp. UWO241 were fractionated using Suc density centrifugation. B to E, SDS-PAGE profiles of purified major complexes were Coomassie stained (B and C) and immunoblotted with P-Thr antibodies (D and E). F to I, 77K fluorescence emission spectra of intact thylakoid membranes (F and G) were compared to those of purified fractions of LHCII, PSII, PSI, and the SC in *C. reinhardtii* 1690 (H) and *Clamydomonas sp.* UWO241 (I). Chl fluorescence was excited at 436 nm.

the PSI complex (PsaA) were primarily associated with the stromal fraction, whereas PSII (PsbA) was primarily associated with the granal fraction in *C. reinhardtii* (Fig. 10). Although the PSI complex was primarily associated with the stromal fraction, both the $Cytb_6/f$ and PSII were relatively evenly distributed between all three fractions (granal, margin, and stromal) in UWO241 regardless of the salt concentration of the growth medium, indicating an altered distribution and organization of PSI and PSII within its thylakoid membrane relative to that of *C. reinhardtii* (Fig. 10). However, Lhcbm appeared to be relatively evenly distributed in all three thylakoid fractions in *C. reinhardtii* as well as in UWO241 (Fig. 10). As an additional control, we performed digitonin fractionation of *C. reinhardtii* and UWO241 thylakoids isolated from cells grown at the same temperature (16°C; Supplemental Fig. S7). Supplemental Figure S7 illustrates that the differential PsaA/PsbA ratios observed between *C. reinhardtii* and UWO241 thylakoid fractions were comparable whether cells were grown at their optimal temperatures of either 5°C or 28°C for UWO241 and *C. reinhardtii*, respectively (Fig. 10), or at a common but suboptimal growth temperature of 16°C (Supplemental Fig. S7).

Transmission electron microscopy of intact cells of UWO241 grown at LS (70 mM; Fig. 11, E and F) indicated thylakoid membrane appression comparable to that observed in *C. reinhardtii* (Fig. 11, A and B, respectively). However, growth of UWO241 under its natural, HS regime (700 mM) appeared to induce swelling of the thylakoid lumen (Fig. 11, C and D). The latter may indicate an osmotic effect of the unusually HS concentration to which UWO241 is naturally exposed.

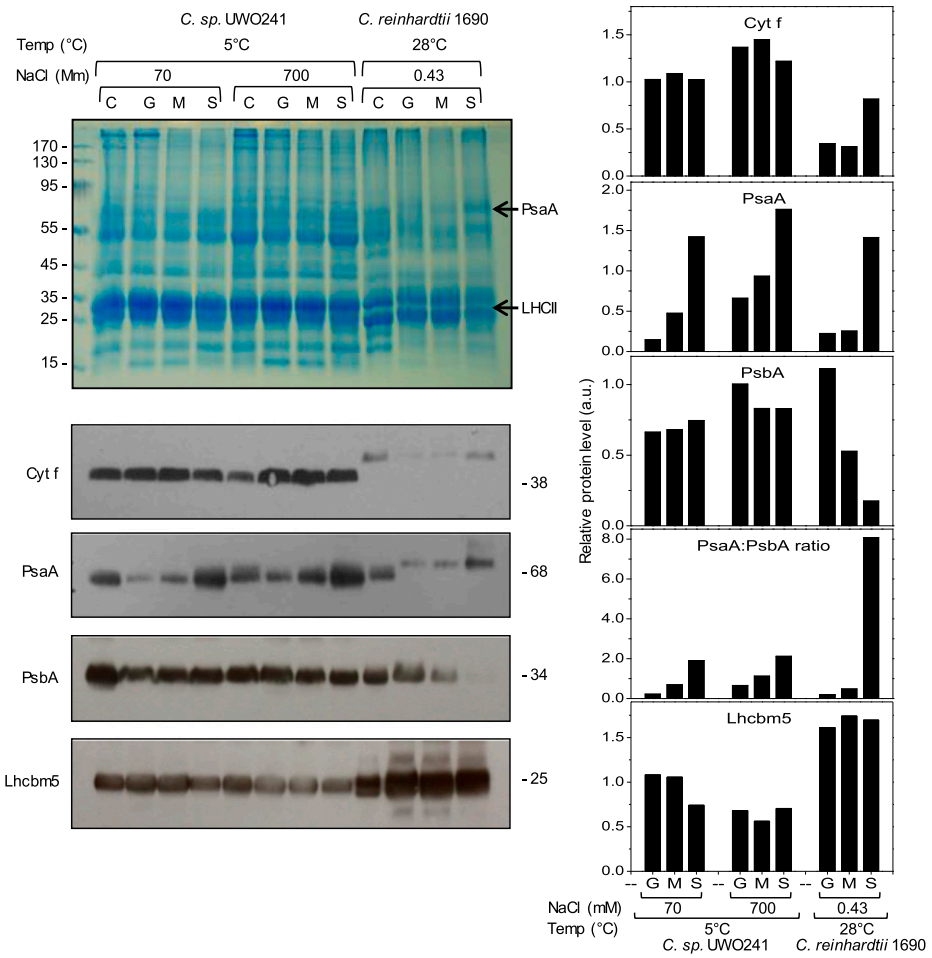

Figure 10. Top left, Cultures of *Clamydomonas* sp. UWO241 and *C. reinhardtii* 1690 were grown at 5°C (70 and 700 mM NaCl) and 23°C (0.43 mM NaCl), respectively. Isolated thylakoid membranes (C) were treated with digitonin and subfractionated into grana (G), margin (M), and stroma (S) using differential centrifugation. Bottom left, Fractions were subjected to SDS-PAGE and loaded on a chlorophyll basis. Cytochrome *f* (Cyt *f*), marker proteins for PSI (PsaA), PSII (PsbA), and Lhcbm5 were immunodetected using specific antibodies. Right, Relative protein concentrations were analyzed with ImageJ. The data reflect typical results of three replicates from a single experiment.

DISCUSSION

A highlight of this study is the observation that UWO241 possesses active cold-adapted thylakoid protein kinases. The extent of the light-dependent thylakoid polypeptide phosphorylation as detected by ^{33}P-labeling is differentially temperature sensitive and highest near or at the optimal growth temperature for both *C. reinhardtii* and UWO241 (Figs. 1 and 2). As expected, the extent of protein phosphorylation in *C. reinhardtii* was inhibited when performed at an incubation temperature (8°C) that is well below its optimal growth temperature (28°C). In contrast, the extent of polypeptide phosphorylation was inhibited in UWO241 when performed at 23°C (Fig. 2), a temperature that inhibits growth of UWO241 (Possmayer et al., 2011). These results are consistent with the evolution of UWO241 as a psychrophile adapted to its low temperature-HS Antarctic environment, and they represent an example of psychrophilic Stt7 and Stl1 thylakoid protein kinases.

More detailed analyses of the structure of these thylakoid protein kinases indicated that the kinase domain of the Stt7 kinase from UWO241 exhibits structural alterations compared to that of *C. reinhardtii* (Figs. 3–5, Supplemental Figs. S3S–S5) that may predispose it to function maximally at low temperature and may contribute to its relative insensitivity to the protein kinase inhibitor staurosporine. Thus, we suggest that the Stt7 and Stl1 kinases in UWO241 appear to be examples of cold-adapted, membrane-bound enzymes that function optimally at low temperature and exhibit a decrease in activity at moderate to high temperatures (De Maayer et al., 2014; Åquist et al., 2017). A unique feature that we identified for the Stt7 kinase from UWO241 is the absence of an autophosphorylation domain (Supplemental Fig. S3, A and B). Stt7-dependent autophosphorylation and Stt7-dependent phosphorylation of Stl1 were detected during state transitions in *C. reinhardtii* (Lemeille et al., 2010; Lemeille and Rochaix, 2010). Although the precise function of the Stt7 autophosphorylation domain remains equivocal in *C. reinhardtii*, it has been suggested that this domain may regulate the efficiency and kinetics of Stt7 and that Stt7 acts upstream of Stl1 in a signal transduction pathway (Lemeille et al., 2010; Lemeille and Rochaix, 2010). In addition, UWO241 encodes two Stl1 homologs (*Stl1-A* and *Stl1-B*), whereas this enzyme is encoded by a single gene in *C. reinhardtii* (Supplemental Figs. S3 and S4; Supplemental Table S1). We suggest that the latter is probably due to a gene duplication event.

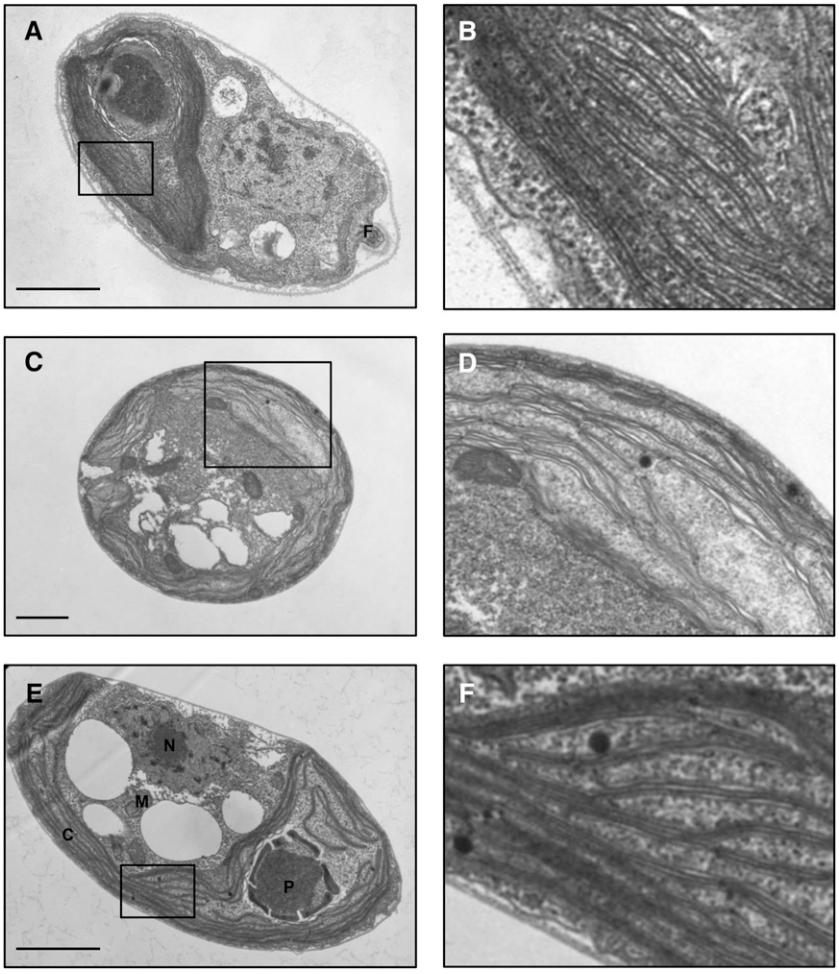

Figure 11. Typical electron micrographs of *C. reinhardtii* and *Clamydomonas* sp. UWO241 are shown. The images in the right column are magnifications of the boxed areas in the left column for midlog phase cells of *C. reinhardtii* grown in BBM at 23°C (A and B), UWO241 grown in HS (700 mM NaCl) at 5°C (C and D), and UWO241 grown in LS (70 mM NaCl) at 5°C (E and F). Scale bars = 1.0 μm. C, chloroplast; N, nucleus; M, mitochondrion; P, pyrenoid.

Contrary to our previous reports (Morgan-Kiss et al., 2002b; Takizawa et al., 2009), we show here that UWO241 not only phosphorylates LHCII, based on ^{33}P-labeling, but is also able to undergo qualitatively novel state transitions based on 77K fluorescence emission spectra in response to DCMU or DBMIB treatment (Fig. 6; Table 1). As a consequence, modulation of PSI/PSII energy distribution required deconvolution to detect a change in this ratio (Figs. 2 and 6) due to the absence of the prominent 77K emission band normally observed at 712 nm. We suggest that the necessity for deconvolution of 77K fluorescence emission spectra to quantify state transitions, as well as the use of ^{33}P-labeling to confirm phosphorylation of LHCII, accounts for our previous mistaken conclusion that UWO241 is unable to undergo state transitions (Morgan-Kiss et al., 2002b).

UWO241 exhibits an atypical modulation of PSI/PSII energy distribution that remains qualitatively distinct from the traditional state transition response associated with *C. reinhardtii* (Fig. 6). Furthermore, dark/light transitions at its optimal growth temperature had minimal effects on PSII/PSI energy distribution in UWO241 (Fig. 7), whereas the thylakoid architecture (Fig. 11), the PSII/PSI energy distribution (Fig. 7), and the quantum efficiency of PSI (Supplemental Fig. S6) were sensitive to salt concentration. However, the extent of LHCII phosphorylation as assessed by ProQ Diamond staining (Supplemental Fig. S1) indicated that LHCII phosphorylation in UWO241 appeared to be insensitive to salt concentration, which is contrary to the results for the halotolerant green alga *Dunaliella salina* (Liu and Shen, 2004; Chen et al., 2010). PSI/PSII energy distribution is clearly sensitive to NaCl concentration in UWO241 (Fig. 7, Table 2) but LHCII phosphorylation is not (Supplemental Fig. S1). A unique feature of UWO241 is that salt-dependent modulation of PSI/PSII energy distribution in UWO241 does not appear to be correlated with salt-dependent phosphorylation of LHCII. Thus, the results presented here indicate that modulation of PSI/PSII energy distribution in UWO241 does not appear to be dependent on a LHCII phosphorylation-dependent mechanism normally observed in the model green alga *C. reinhardtii* (Delosme et al., 1996; Takahashi et al., 2006; Eberhard et al., 2008; Rochaix, 2011, 2014).

The mechanism regulating state transitions is, by and large, considered to be governed by a reversible, LHCII phosphorylation-dependent mechanism in plants and green algae (Fork and Satoh, 1986; Salehian and Bruce,

1992; Eberhard et al., 2008; Papageorgiou and Govindjee, 2011; Rochaix, 2011, 2014; Tikkanen and Aro, 2014; Ünlü et al., 2014; Ueno et al., 2016). The reversible LHCII phosphorylation associated with this physiological process is considered to be regulated by the thylakoid protein kinases Stt7 and Stl1 in *C. reinhardtii* and their orthologs, STN7 and STN8, in Arabidopsis (*Arabidopsis thaliana*; Rochaix, 2011, 2014; Wunder et al., 2013). The protein kinase activities are sensitive to the reduction state of the intersystem photosynthetic electron transport chain (Allen et al., 1981; Oxborough et al., 1987; Bennett, 1991; Allen, 1992; Zer and Ohad, 2003).

Historically, the discovery of the state transition phenomenon (Bonaventura and Myers, 1969; Murata, 1969) represented the basis of a mechanism by which a balanced excitation of PSII and PSI could be fulfilled by energy spillover between the two photosystems to ensure optimal rates of photosynthetic electron transport despite their extensive physical separation and different spectral properties (Fork and Satoh, 1986; Papageorgiou and Govindjee, 2011). Initially, the energy spillover mechanism was proposed to account for changes in PSII/PSI energy distribution associated with state transitions. This mechanism is associated with cation-induced thylakoid membrane stacking/unstacking as a function of in vitro salt concentrations, which induces changes in PSII/PSI lateral heterogeneity such that energy transfer or spillover is enhanced between PSII and PSI due to a reduction in the spatial distance between PSII and PSI complexes (Wollman and Diner, 1980; Barber, 1982; Fork and Satoh, 1986; Dau and Hansen, 1988; Papageorgiou and Govindjee, 2011; Tikkanen and Aro, 2012, 2014; Grieco et al., 2015).

Slavov et al. (2013) employed ultrafast fluorescence spectroscopy to examine quenching of excessive excitation energy during desiccation in the alga associated with the thalli of the lichen *Parmelia sulcata*. Desiccation induced a thylakoid reorganization of PSII and PSI such that the PSII and PSI units were in direct contact, which allows PSII to transfer energy directly to PSI through a spillover process, which in turn protects PSII and PSI from chronic photodamage. This novel PSII-PSI spillover mechanism appears to also exist in the dinoflagellate *Symbiodinium* during heat stress (Slavov et al., 2016). However, no biochemical evidence for the requirement of protein phosphorylation in the regulation of the PSII-PSI spillover mechanism was examined in either of those studies.

A feature of cold adaptation in UWO241 is the apparent reorganization of PSII and PSI units relative to those in *C. reinhardtii* based on digitonin fractionation of thylakoid membranes combined with immunodetection of specific thylakoid complexes, which indicated a decrease in lateral heterogeneity between grana and stromal lamellae in UWO241 compared to *C. reinhardtii* (Fig. 10). In addition, although a PSI 77K fluorescence emission maximum is observed at 712 nm after Suc gradient purification of UWO241 PSI (Fig. 9I), this emission band is difficult to detect because it appears to be blue-shifted by 5–6 nm in isolated thylakoids (Fig. 9G) as well as intact cells of UWO241 (Figs. 6, B and D, and 7). Deconvolution of the 77K fluorescence emission spectra of UWO241 was necessary to detect a putative PSI emission band at 706–707 nm (Table 2). These data support our contention that PSII/PSI organization has been altered in UWO241 relative to *C. reinhardtii* and has resulted in a strong quenching capacity of excess excitation energy in UWO241, as reported previously (Szyszka et al., 2007). However, energy quenching through the constitutive energy quenching process (φNO) is favored in UWO241 (Szyszka et al., 2007) over the expected regulated and inducible process (φnonphotochemical quenching) governed by the xanthophyll cycle (Demmig-Adams et al., 1999, 2014; Niyogi, 1999; Murchie et al., 2009; Ruban, 2016). The mechanism(s) that govern energy quenching via processes involved in φNO has been suggested to occur through PSII reaction center quenching (Ivanov et al., 2008), but the underlying mechanism remains equivocal. We suggest that the reorganization of the photosynthetic apparatus of UWO241 with respect to PSII and PSI units coupled with its strong quenching capacity (Szyszka et al., 2007) may reflect a PSII-PSI spillover mechanism similar to that reported by Slavov et al. (2013, 2016). However, further experimentation is required to differentiate the potential contribution of the LHCII phosphorylation-dependent mechanism for state transitions versus the PSII-PSI spillover mechanism.

UWO241 PSI exists as an independent pigment-protein complex as well as a component of a PSI-Cyb_6/f SC with a polypeptide complement that is distinct from that of *C. reinhardtii* (Fig. 9). Nano liquid chromatography electrospray ionization tandem mass spectrometry analyses identified PsaA, PsaB, and $Cytb_6/f$ as major components of this PSI-$Cytb_6/f$ SC (Szyszka-Mroz et al., 2015). Although ^{33}P-labeling (Fig. 1A, arrows) and P-Thr immunodetection (Fig. 9, D and E) indicated that subunits of the UWO241 PSI-$Cytb_6/f$ SC are phosphorylated, this is not the case for the corresponding subunits from *C. reinhardtii*. Nano liquid chromatography electrospray ionization tandem mass spectrometry identified the phosphorylated subunits of the UWO241 PSI SC to be two PsbP-like proteins of 17 kD and an ATP-dependent Zn-metalloprotease (Szyszka-Mroz et al., 2015). The stability of the PSI-$Cytb_6/f$ SC is dependent upon the phosphorylation status of these subunits as well as the [NaCl] of the growth medium (Szyszka-Mroz et al., 2015). Recently, it was reported that the stability of the UWO241 SC also appears to be sensitive to the [Fe] of the growth medium (Cook et al., 2019). The role of this novel PSI-$Cytb_6/f$ complex and its phosphorylation status in governing PSI/PSII energy distribution and state transitions requires further investigation.

We suggest that thylakoid membrane remodelling coupled with cold adaptation of the STT7 protein kinase has modified the mechanism that governs PSI/PSII

energy distribution and energy quenching in the psychrophile UWO241 compared to the model green alga *C. reinhardtii*. This appears to be due to its adaptation to an extreme environment of low temperature combined with unusually HS. We suggest that the study of nonmodel life forms such as *Chlamydomonas* sp. UWO241, Antarctic terrestrial plants (Bravo et al., 2001, 2007; Bascuñán-Godoy et al., 2012), and terrestrial surface soil photosynthetic microorganisms (Ji et al., 2017) adapted to such extreme polar conditions will provide new insights into the mechanisms that underlie previously unrealized photosynthetic plasticity as a consequence of the evolution of life at the edge.

MATERIALS AND METHODS

Growth Conditions

The mesophiles *Chlamydomonas reinhardtii* 1690 and *Chlamydomonas raudensis* SAG49.72 were grown axenically in Bold's basal medium (BBM), whereas the psychrophile *Chlamydomonas* sp. UWO241 was grown in BBM supplemented with either HS (700 mM NaCl) or LS (70 mM NaCl). All cultures were aerated continuously under ambient CO_2 conditions in 4L glass Pyrex bottles. A growth irradiance of 150 μmol photons m^{-2} s^{-1} was generated by fluorescent tubes (Sylvania CW-40) and measured with a quantum sensor attached to a radiometer (model LI-189; Li-Cor). Cultures of *C. reinhardtii* and *C. raudensis* were grown at 23°C, whereas those of UWO241 were grown at 5°C. Midlog phase cells were used in all experiments.

Electron Microscopy

Cells of *C. reinhardtii* 1690 were grown in BBM whereas UWO241 cells were grown in BBM supplemented with either HS or LS as described above. Cultures were centrifuged, fixed with equal parts fresh 4% (v/v) glutaraldehyde and 2% (v/v) osmium tetroxide buffered with 0.1 M sodium cacodylate, pH 6.8, and stained with 2% (v/v) osmium tetroxide as described previously in Pocock et al. (2004). Fixed cells were collected by centrifugation and resuspended in agar, stained with 3% (w/v) uranyl acetate and dehydrated with acetone. The agar blocks were infiltrated and embedded with Lipon-Araldite according to Pocock et al. (2004). All samples were processed and captured using a Philips CM10 transmission electron microscope (Philips Research Eindhoven) operating at 80 Kv.

Isolation of Purified LHCII Complexes

Cells were disrupted by passing a suspension through a chilled French press at 6000 lb in^{-2}, twice. Thylakoid membranes were purified through a Suc step gradient centrifugation procedure as described previously in Chua and Bennoun (1975). Purified thylakoid membranes were resuspended in dH_2O at a chlorophyll concentration of 0.9 mg/mL and solubilized with 1% (w/v) n-dodecyl β-D-maltoside on ice for 25 min and centrifuged to remove unsolubilized material. Solubilized thylakoid membranes were loaded on a continuous 1.3–0.1 M Suc density gradient and ultracentrifuged as previously described in Takahashi et al. (2006). All isolation buffers were supplemented with 20 mM NaF. Separated bands containing LHCII were isolated, diluted 3 times with 20 mM HEPES, pH 7.5, and centrifuged at 150,000*g* for 8 h.

Low-Temperature (77K) Chlorophyll Fluorescence

Samples of *C. reinhardtii* 1690 and UWO241 whole cells and purified LHCII fractions were resuspended to a chlorophyll concentration between 5 and 10 μg/mL in the presence of 10% (v/v) glycerol. Samples were frozen in NMR tubes with liquid nitrogen and excited at 436 nm (Quanta Master, Photon Technology International). Corrected emission spectra were collected between 650 and 800 nm using a 814 Photomultiplier Detection System fluorometer (Photon Technology International), with Felix32 Analysis Module (V1.2) software (Photon Technology International). A slit width of 4 nm was used for both excitation and emission. Spectra were normalized to a maximal signal value of 1.0 for comparison. All spectra represent an average of at least three independent experiments with three scans in each experiment.

The low-temperature (77K) chlorophyll fluorescence of *C. reinhardtii* 1690 and UWO241 cells cultivated at different growth conditions were further analyzed via decomposition of the emission spectra. Decomposition analysis of the fluorescence emission spectra in terms of five Gaussian bands was carried out by a nonlinear least-squares algorithm that minimizes the χ^2 function using a Microcal Origin Version 7.0 software package (Microcal Software). The fitting parameters for the five Gaussian components, that is, position, area, and full width at half maximum (FWHM), were free-running parameters (Morgan-Kiss et al., 2002a).

PSI Measurements

In vivo far-red (FR) light induced redoxkinetics of P700 in *C. reinhardtii* 1690 and UWO241 cells were determined under ambient O_2 and CO_2 conditions and the corresponding growth temperature of each strain using a PAM-101 modulated fluorometer (Heinz Walz GmbH) equipped with a dual-wavelength emitter-detector ED-P700DW unit and PAM-102 units (Klughammer and Schreiber, 1991), as described in detail by Ivanov et al. (2000). FR light (λ_{max} = 715 nm, 10 W m^{-2}, Schott filter RG 715) was provided by an FL-101 light source (American Lighting). The redox state of P700 was evaluated as the absorbance change around 820 nm ($\Delta A_{820-860}$) in a custom-designed cuvette. The capacity of PSI cyclic electron (e^-) flow was determined as the half-time for the dark decay of the $P700^+$ signal (Herbert et al., 1995; Ivanov et al., 2000, 2012).

The effective absorption cross section (σ) of PSI in *C. reinhardtii* 1690 and UWO241 strains was estimated in DCMU (10 μM) pretreated dark-adapted (30 min) whole cells. The absorption changes of P700 ($A_{820-860}$) were examined with an ED-P700DW detector (Heinz Walz GmbH) after excitation with a 10 μs flash with varying intensity from a xenon pump flash lamp/control unit, XE-STC, as described in Ivanov et al. (2006). Relative antenna size was determined by fitting the curves with the cumulative Poisson single hit probability distribution (Mauzerall and Greenbaum, 1989; Samson and Bruce, 1995).

SDS-PAGE and Immunoblotting

Purified thylakoid membranes and LHCII fractions isolated by Suc density gradient centrifugation were solubilized with 1% (w/v) SDS and 1% (v/v) β-mercaptoethanol and loaded on an equal chlorophyll basis. Electrophoresis was performed using a Mini-Protean II apparatus (Bio-Rad) with an 18% (w/v) polyacrylamide resolving gel containing 6 M urea, 0.66 M Tris (pH 8.8) and an 8% (w/v) polyacrylamide stacking gel containing 0.125 M Tris (pH 6.8), using the Laemmli buffer system (Laemmli, 1970). Proteins separated by SDS-PAGE were stained with Coomassie blue or transferred electrophoretically to nitrocellulose membranes (0.2 μm pore size; Bio-Rad) at 100 V for 1 h at 5°C. The membranes were preblocked with a Tris-buffered salt (20 mM Tris, pH 7.5 and 150 mM NaCl) containing 3% (w/v) bovine serum albumin or 5% (w/v) milk powder and 0.01% (v/v) Tween 20. Membranes were probed with antibodies specific for the Stt7 kinase (1:3000 dilution), PsbA (D1 protein; 1:2,000 dilution), or *Chlamydomonas* LHCII antibodies Lhcb4, Lhcb5, and Lhcbm5 from Agrisera (1:5,000 dilution). Immunodetection of phosphorylation was performed using P-Thr, phospho-Ser, and phosphotyrosine antibodies (Zymed Laboratories) at 1:500 dilution. After incubation with secondary antibodies conjugated with horseradish peroxidase (Sigma), the antibody-protein complexes were visualized using ECL chemiluminescent detection reagents (GE Healthcare) and performed according to the manufacturer's instructions.

^{33}P Labeling of Isolated Thylakoid Membranes

Thylakoid membranes were purified through a Suc step gradient centrifugation procedure as described above (Chua and Bennoun, 1975). Purified thylakoids were resuspended at a chlorophyll concentration of 0.4 mg/mL in 25 mM Tricine (pH 7.8), 100 mM sorbitol, 20 mM NaCl, and 5 mM $MgCl_2$ as described by Carlberg et al. (1999). Membranes were phosphorylated in the presence of 0.25 mM [γ-^{33}P]ATP containing 0.02 mCi/mg of chlorophyll. Phosphorylation was measured at either 23°C or 8°C, under irradiance of either 200 μmol photons m^{-2} s^{-1} or in darkness. The reaction was terminated by the

addition of 50 mM EDTA (pH 8) and 20 mM NaF, followed by rapid centrifugation and resuspension of the membranes in solubilization buffer containing 4% (w/v) SDS and 100 mM dithiothreitol. Proteins were resolved on 12.5% (w/v) SDS-PAGE gels, transferred electrophoretically onto nitrocellulose membranes at 100 V for 1 h at 5°C, and exposed to film, as described in "SDS-PAGE and Immunoblotting". Subsequently, the same nitrocellulose membranes used to generate the autoradiographs were stained with Ponceau S stain (0.1% (w/v) and 5.0% (w/v) acetic acid for 30 min and rinsed with dH_2O.

ProQ Diamond Phosphoprotein Gel Staining

Thylakoid membranes and LHCII complexes were purified using Suc gradient centrifugation as described above, and the resulting fractions were resolved by SDS-PAGE. ProQ Diamond stain was used according to the manufacturer's instructions (Molecular Probes). Stained gels were visualized using a Bio-Rad VersaDoc Imaging System. Subsequently, ProQ Diamond-stained gels were stained with Coomassie stain to visualize total proteins.

Digitonin Subfractionation of Thylakoid Membranes

Digitonin solubilization was performed as described (Barbato et al., 2000). Briefly, thylakoid membranes (0.4 mg chlorophyll/mL) were treated with 0.5% (w/v) digitonin for 30 min on ice. Unsolubilized material was removed by centrifugation at 4000*g* for 5 min, and granum-, margin-, and stroma-enriched fractions were isolated by centrifugation at 10,000*g* (10 min), 40,000*g* (30 min), and 100,000*g* (90 min), respectively. Fractions were subjected to SDS-PAGE and immunoblotting.

Complementary DNA Library Construction

A modified cetyl-trimethyl-ammonium bromide protocol (Doyle, 1991) was used to extract RNA from UWO241 cells ground in liquid nitrogen. Briefly, 2 times (v/w) cetyl-trimethyl-ammonium bromide buffer at 60°C was added to tissue, vortexed, and incubated for 10 min at 60°C. Following two chloroform extractions, nucleic acids were precipitated with an equal volume of isopropanol. Nucleic acids were resuspended in diethyl pyrocarbonate-treated water and RNA was precipitated with an equal volume of 4 M LiCl. Following resuspension, contaminating polysaccharides were precipitated by adding one-thirtieth volume 3 M sodium acetate (pH 5.2) and one-tenth volume 100% ethanol, incubated on ice for 30 min, and centrifuged for 30 min (Asif et al., 2000). The supernatant was transferred to a new tube, and RNA was precipitated with sodium acetate and ethanol, the pellet was washed with 70% (v/v) ethanol and resuspended in diethyl pyrocarbonate-treated water.

Messenger RNA was isolated from total RNA using a Dynabeads mRNA Purification Kit (Life Technologies) according to the manufacturer's instructions. A complementary DNA (cDNA) library was constructed with a Lambda Zap Gigapack Gold III cDNA Library Construction Kit (Agilent) according to the manufacturer's instructions. Treatment of mRNA with methylmercury hydroxide was performed prior to reverse transcription.

Cloning of Stt7 and Stl1 from UWO241

The genome and transcriptome of UWO241 were sequenced and assembled as described previously (Cvetkovska et al., 2018). These datasets were screened for the presence of sequences resembling *Stl1* and *Stt7* using known conserved regions within *C. reinhardtii Stt71/Stl1* nucleotide sequences available through the National Center for Biotechnology Information database. Partial sequences from UWO241 were obtained and used to design primers for cDNA library screening. Two gene-specific primers were used to isolate the full-length cDNA in combination with two vector-specific T3/T7 primers for each gene, as indicated below. Taq DNA polymerase (New England BioLabs) was used in PCR reactions to amplify the sequences. In the case of Stt77, the sequence identity was confirmed by preforming RACE-PCR using the SMARTer RACE 5′/3′ Kit (Clontech) according to manufacturer's instructions.

PCR samples were resolved on 1% (w/v) agarose gels stained with ethidium bromide. Bands were excised from the gel and purified with a gel extraction kit (Qiagen) following the manufacturer's instructions, and DNA fragments were submitted for sequencing reactions (Robarts Research Institute). Overlapping gene sequences were combined and used to generate the full Stt7 and Stl1 amino acid sequences.

Bioinformatics Analysis of Nucleotide and Protein Sequences

The UWO241 genome assembly was screened for the presence of *Stt7* and *Stl1* using the transcript sequences obtained by cloning as the query. Genomic sequences with a high degree of identity (E-value cutoff 10^{-30}) were obtained and annotated using Geneious V9.1 (Biomatters). The coding sequences were extracted and were used to confirm the nucleotide sequence of the cloned transcripts and predict the amino acid sequence and M_r of the encoded proteins. Sequence alignments were performed using ClustalW (Sievers et al., 2011) implemented through Geneious V9.1.

Protein structure predictions were performed with Protein Homology/analog Y Recognition Engine v2.0 (Phyre2; Kelley et al., 2015), available on the web (http://www.sbg.bio.ic.ac.uk/Phyre2/). Molecular graphics and analyses were performed with the University of California San Francisco Chimera package (Pettersen et al., 2004).

Accession Numbers

Sequence data from this article can be found in the GenBank/EMBL data libraries under accession numbers listed in Supplemental Table S3.

Supplemental Data

The following supplemental information is available:

Supplemental Figure S1. Thylakoid membrane proteins of *C. reinhardtii* and *Clamydomonas* sp. UWO241 grown in LS and HS.

Supplemental Figure S2. Purified LHCII complexes of *C. reinhardtii* 1690 and *Clamydomonas* sp. UWO241 isolated in the presence of the kinase inhibitor staurosporine or the phosphatase inhibitor NaF.

Supplemental Figure S3. Predicted secondary structures of Stt7 in *C. reinhardtii* and UWO241.

Supplemental Figure S4. Predicted secondary structures of Stl1 in *C. reinhardtii* and UWO241.

Supplemental Figure S5. A graphical representation of the gene structure of Stt7 and Stl1 in *C. reinhardtii* and *Clamydomonas* sp. UWO241.

Supplemental Figure S6. Flash-saturation curves of the relative extent of P700 photooxidation ($P700^+$).

Supplemental Figure S7. Digitonin fractionation of thylakoid membranes from cultures of *Clamydomonas* sp. UWO241 and *C. reinhardtii* 1690.

Supplemental Table S1. A comparison of the gene structure of the chloroplast kinases, Stt7 and Stl1.

Supplemental Table S2. Primer design for cDNA library screening of UWO241 *Stl1* and *Stt7* sequences.

Supplemental Table S3. GenBank accession numbers.

ACKNOWLEDGMENTS

The authors are grateful to Professor R. Bassi for the gift of *C. reinhardtii* Stt7 antibodies.

Received April 7, 2019; accepted April 9, 2019; published April 24, 2019.

LITERATURE CITED

Allen JF (1992) Protein phosphorylation in regulation of photosynthesis. Biochim Biophys Acta **1098:** 275–335

Allen JF, Bennett J, Steinback KE, Arntzen CJ (1981) Chloroplast protein phosphorylation couples plastoquinone redox state to distribution of excitation energy between photosystems. Nature **291:** 25–29

Åquist J, Isaksen GV, Brandsdal BO (2017) Computation of enzyme cold adaptation. Nat Rev Chem **1:** 0051

Aro EM, Rokka A, Vener AV (2004) Determination of phosphoproteins in higher plant thylakoids. Methods Mol Biol **274:** 271–285

Asif MH, Dhawan P, Nath P (2000) A simple procedure for the isolation of high quality RNA from ripening banana fruit. Plant Mol Biol Report **18:** 109–115

Barbato R, Bergo E, Szabò I, Dalla Vecchia F, Giacometti GM (2000) Ultraviolet B exposure of whole leaves of barley affects structure and functional organization of photosystem II. J Biol Chem **275:** 10976–10982

Barber J (1982) Influence of surface charges on thylakoid structure and function. Annu Rev Plant Physiol **33:** 261–295

Bascuñán-Godoy L, Sanhueza C, Cuba M, Zuñiga GE, Corcuera LJ, Bravo LA (2012) Cold-acclimation limits low temperature induced photoinhibition by promoting a higher photochemical quantum yield and a more effective PSII restoration in darkness in the Antarctic rather than the Andean ecotype of *Colobanthus quitensis* Kunt Bartl (Cariophyllaceae). BMC Plant Biol **12:** 114–128

Bassi R, Soen SY, Frank G, Zuber H, Rochaix JD (1992) Characterization of chlorophyll *a/b* proteins of photosystem I from *Chlamydomonas reinhardtii*. J Biol Chem **267:** 25714–25721

Bennett J (1991) Protein phosphorylation in green plant chloroplasts. Annu Rev Plant Physiol Plant Mol Biol **42:** 281–311

Bielewicz S, Bell E, Kong W, Friedberg I, Priscu JC, Morgan-Kiss RM (2011) Protist diversity in a permanently ice-covered Antarctic lake during the polar night transition. ISME J **5:** 1559–1564

Bonaventura C, Myers J (1969) Fluorescence and oxygen evolution from *Chlorella pyrenoidosa*. Biochim Biophys Acta **189:** 366–383

Bossemeyer D (1994) The glycine-rich sequence of protein kinases: A multifunctional element. Trends Biochem Sci **19:** 201–205

Bravo LA, Ulloa N, Zuniga GE, Casanova A, Corcuera LJ, Alberdi M (2001) Cold resistance in Antarctic angiosperms. Physiol Plant **111:** 55–65

Bravo LA, Saavedra-Mella FA, Vera F, Guerra A, Cavieres LA, Ivanov AG, Hüner NPA, Corcuera LJ (2007) Effect of cold acclimation on the photosynthetic performance of two ecotypes of *Colobanthus quitensis* (Kunth) Bartl. J Exp Bot **58:** 3581–3590

Carlberg I, Rintamäki E, Aro EM, Andersson B (1999) Thylakoid protein phosphorylation and the thiol redox state. Biochemistry **38:** 3197–3204

Chen W, Jin N, Shi Y, Su Y, Fei B, Li W, Qiao D, Cao Y (2010) Coordinate expression of light-harvesting chlorophyll *a/b* gene family of photosystem II and chlorophyll *a* oxygenase gene regulated by salt-induced phosphorylation in *Dunaliella salina*. Photosynthetica **48:** 355–360

Chrismas NA, Anesio AM, Sánchez-Baracaldo P (2015) Multiple adaptations to polar and alpine environments within cyanobacteria: A phylogenomic and Bayesian approach. Front Microbiol **6:** 1070

Chua NH, Bennoun P (1975) Thylakoid membrane polypeptides of *Chlamydomonas reinhardtii*: Wild-type and mutant strains deficient in photosystem II reaction center. Proc Natl Acad Sci USA **72:** 2175–2179

Cook G, Teufel A, Kalra I, Wang X, Priscu J, Morgan-Kiss R (2019) The Antarctic psychrophiles *Chlamydomonas* sp. UWO241 and ICE-MDV exhibit differential restructuring of photosystem I in response to iron. Photosyn Res doi:10.1007/s11120-019-00621-0

Cvetkovska M, Hüner NPA, Smith DR (2017) Chilling out: The evolution and diversification of psychrophilic algae with a focus on Chlamydomonadales. Polar Biol **40:** 1169–1184

Cvetkovska M, Szyszka-Mroz B, Possmayer M, Pittock P, Lajoie G, Smith DR, Hüner NPA (2018) Characterization of photosynthetic ferredoxin from the Antarctic alga *Chlamydomonas* sp. UWO241 reveals novel features of cold adaptation. New Phytol **219:** 588–604

Cvetkovska M, Orgnero S, Hüner NPA, Smith DR (2019) The enigmatic loss of light-independent chlorophyll biosynthesis from a polyextremophilic green alga (*Chlamydomonas* sp. UWO241) living in a light-limited environment. New Phytol **222:** 651–656

Dau H, Hansen UP (1988) The involvement of spillover changes in State 1-State 2 transitions in intact leaves at low light intensities. Biochim Biophys Acta **934:** 156–159

De Bondt HL, Rosenblatt J, Jancarik J, Jones HD, Morgan DO, Kim SH (1993) Crystal structure of cyclin-dependent kinase 2. Nature **363:** 595–602

Delosme R, Olive J, Wollman FA (1996) Changes in light energy distribution upon state transitions: An in vivo photoacoustic study of the wild type and photosynthesis mutants from *Chlamydomonas reinhardtii*. Biochim Biophys Acta **1273:** 150–158

De Maayer P, Anderson D, Cary C, Cowan DA (2014) Some like it cold: Understanding the survival strategies of psychrophiles. EMBO Rep **15:** 508–517

Demmig-Adams B, Adams WW, Ebbert V, Logan BA (1999) Ecophysiology of the xanthophyll cycle. In HA Frank, AJ Young, G Britton, RJ Cogdell, eds, The Photochemistry of Carotenoids, **Vol 8**. Kluwer Academic Publishers, Dordrecht, the Netherlands, pp 245–269

Demmig-Adams B, Stewart JJ, Burch TA, Adams III WW (2014) Insights from placing photosynthetic light harvesting into context. J Phys Chem Lett **5:** 2880–2889

Dolhi JM, Maxwell DP, Morgan-Kiss RM (2013) The Antarctic *Chlamydomonas raudensis*: An emerging model for cold adaptation of photosynthesis. Extremophiles **17:** 711–722

Doyle J (1991) DNA protocols for plants. In G Hewitt, AB Johnston, JP Young, eds, Molecular Techniques in Taxonomy. Springer, Berlin/Heidelberg, pp 283–293

Eberhard S, Finazzi G, Wollman FA (2008) The dynamics of photosynthesis. Annu Rev Genet **42:** 463–515

Feller G, Gerday C (2003) Psychrophilic enzymes: Hot topics in cold adaptation. Nat Rev Microbiol **1:** 200–208

Fork DC, Satoh K (1986) The control by state transitions of the distribution of excitation energy in photosynthesis. Annu Rev Plant Physiol **37:** 335–361

Grieco M, Suorsa M, Jajoo A, Tikkanen M, Aro E-M (2015) Light-harvesting II antenna trimers connect energetically the entire photosynthetic machinery—including both photosystems II and I. Biochim Biophys Acta **1847:** 607–619

Gudynaite-Savitch L, Gretes M, Morgan-Kiss RM, Savitch LV, Simmonds J, Kohalmi SE, Hüner NPA (2006) Cytochrome *f* from the Antarctic psychrophile, *Chlamydomonas raudensis* UWO 241: Structure, sequence, and complementation in the mesophile, *Chlamydomonas reinhardtii*. Mol Genet Genomics **275:** 387–398

Guo J, Wei X, Li M, Pan X, Chang W, Liu Z (2013) Structure of the catalytic domain of a state transition kinase homolog from *Micromonas* algae. Protein Cell **4:** 607–619

Hanks SK, Hunter T (1995) Protein kinases 6. The eukaryotic protein kinase superfamily: Kinase (catalytic) domain structure and classification. FASEB J **9:** 576–596

Herbert SK, Martin RE, Fork DC (1995) Light adaptation of cyclic electron transport through Photosystem I in the cyanobacterium *Synechococcus* sp. PCC 7942. Photosynth Res **46:** 277–285

Ivanov AG, Park Y-I, Miskiewicz E, Raven JA, Hüner NPA, Öquist G (2000) Iron stress restricts photosynthetic intersystem electron transport in *Synechococcus* sp. PCC 7942. FEBS Lett **485:** 173–177

Ivanov AG, Krol M, Sveshnikov D, Selstam E, Sandström S, Koochek M, Park Y-I, Vasil'ev S, Bruce D, Öquist G, et al (2006) Iron deficiency in cyanobacteria causes monomerization of photosystem I trimers and reduces the capacity for state transitions and the effective absorption cross section of photosystem I in vivo. Plant Physiol **141:** 1436–1445

Ivanov AG, Hurry V, Sane PV, Oquist G, Hüner NPA (2008) Reaction centre quenching of excess light energy and photoprotection of photosystem II. J Plant Biol **51:** 85–96

Ivanov AG, Allakhverdiev SI, Hüner NPA, Murata N (2012) Genetic decrease in fatty acid unsaturation of phosphatidylglycerol increased photoinhibition of photosystem I at low temperature in tobacco leaves. Biochim Biophys Acta **1817:** 1374–1379

Ji M, Greening C, Vanwonterghem I, Carere CR, Bay SK, Steen JA, Montgomery K, Lines T, Beardall J, van Dorst J, et al (2017) Atmospheric trace gases support primary production in Antarctic desert surface soil. Nature **552:** 400–403

Kelley LA, Mezulis S, Yates CM, Wass MN, Sternberg MJE (2015) The Phyre2 web portal for protein modeling, prediction and analysis. Nat Protoc **10:** 845–858

Kennicutt II MC, Chown SL, Cassano JJ, Liggett D, Massom R, Peck LS, Rintoul SR, Storey JW, Vaughan DG, Wilson TJ, et al (2014) Polar research: Six priorities for Antarctic science. Nature **512:** 23–25

Klughammer C, Schreiber U (1991) Analysis of light-induced absorbency changes in the near-infrared spectral region. 1. Characterization of various components in isolated chloroplasts. Z Naturforsch C **46:** 233–244

Laemmli UK (1970) Cleavage of structural proteins during the assembly of the head of bacteriophage T4. Nature **227:** 680–685

Lemeille S, Rochaix JD (2010) State transitions at the crossroad of thylakoid signalling pathways. Photosynth Res **106:** 33–46

Lemeille S, Willig A, Depège-Fargeix N, Delessert C, Bassi R, Rochaix JD (2009) Analysis of the chloroplast protein kinase Stt7 during state transitions. PLoS Biol **7:** e45

Lemeille S, Turkina MV, Vener AV, Rochaix JD (2010) Stt7-dependent phosphorylation during state transitions in the green alga *Chlamydomonas reinhardtii*. Mol Cell Proteomics **9:** 1281–1295

Liu X-D, Shen Y-G (2004) NaCl-induced phosphorylation of light harvesting chlorophyll *a/b* proteins in thylakoid membranes from the halotolerant green alga, *Dunaliella salina*. FEBS Lett **569:** 337–340

Liu Y, Ding Y, Jian J-C, Wu Z-H, Miao J-L (2011) Prokaryotic expression and its conditional optimization of glutathione reductase gene of antarctic *Chlamydomonas* sp. ICE-L. Oceanol Limnol Sin **42:** 817–821

Lizotte MP, Priscu JC (1992) Spectral irradiance and bio-optical properties in perennially ice covered lakes of the dry valleys (Mcmurdo Sound, Antarctica). In DH Elliot, ed. Contributions to Antarctic Research III, **Vol 57**, AGU Publications, Washington, D.C., pp 1–14

Lizotte MP, Priscu JC (1994) Natural fluorescence and quantum yields in vertically stationary phytoplankton from perennially ice-covered lakes. Limnol Oceanogr **39:** 1399–1410

Lizotte MP, Sharp TR, Priscu JC (1996) Phytoplankton dynamics in the stratified water column of Lake Bonney, Antarctica: Biomass and productivity during the winter-spring transition. Polar Biol **16:** 155–162

Lyon BR, Mock T (2014) Polar microalgae: New approaches towards understanding adaptations to an extreme and changing environment. Biology (Basel) **3:** 56–80

Margesin R, Schinner F, Marx J-C, Gerday C, editors (2007) Psychrophiles: From Biodiversity to Biotechnology. Springer-Verlag, Berlin

Mauzerall D, Greenbaum NL (1989) The absolute size of a photosynthetic unit. Biochim Biophys Acta **974:** 119–140

Mock T, Otillar RP, Strauss J, McMullan M, Paajanen P, Schmutz J, Salamov A, Sanges R, Toseland A, Ward BJ, et al (2017) Evolutionary genomics of the cold-adapted diatom *Fragilariopsis cylindrus*. Nature **541:** 536–540

Moellering ER, Muthan B, Benning C (2010) Freezing tolerance in plants requires lipid remodeling at the outer chloroplast membrane. Science **330:** 226–228

Morgan RM, Ivanov AG, Priscu JC, Maxwell DP, Hüner NPA (1998) Structure and composition of the photochemical apparatus of the antarctic green alga, *Chlamydomonas subcaudata*. Photosynth Res **56:** 303–314

Morgan-Kiss R, Ivanov AG, Williams J, Mobashsher Khan, Hüner NPA (2002a) Differential thermal effects on the energy distribution between photosystem II and photosystem I in thylakoid membranes of a psychrophilic and a mesophilic alga. Biochim Biophys Acta **1561:** 251–265

Morgan-Kiss RM, Ivanov AG, Hüner NPA (2002b) The Antarctic psychrophile, *Chlamydomonas subcaudata*, is deficient in state I-state II transitions. Planta **214:** 435–445

Morgan-Kiss RM, Ivanov AG, Pocock T, Krol M, Gudynaite-Savitch L, Hüner NPA (2005) The Antarctic psychrophile, *Chlamydomonas raudensis* ETTL (UWO241) exhibits a limited capacity to photoacclimate to red light. J Phycol **41:** 791–800

Morgan-Kiss RM, Priscu JC, Pocock T, Gudynaite-Savitch L, Hüner NPA (2006) Adaptation and acclimation of photosynthetic microorganisms to permanently cold environments. Microbiol Mol Biol Rev **70:** 222–252

Murata N (1969) Control of excitation transfer in photosynthesis. I. Light-induced change of chlorophyll *a* fluorescence in *Porphyridium cruentum*. Biochim Biophys Acta **172:** 242–251

Murata N, Los DA (1997) Membrane fluidity and temperature perception. Plant Physiol **115:** 875–879

Murchie EH, Pinto M, Horton P (2009) Agriculture and the new challenges for photosynthesis research. New Phytol **181:** 532–552

Neale PJ, Priscu JC (1995) The photosynthetic apparatus of phytoplankton from a perennially ice-covered Antarctic lake: Acclimation to an extreme shade environment. Plant Cell Physiol **36:** 253–263

Nelson N, Ben-Shem A (2004) The complex architecture of oxygenic photosynthesis. Nat Rev Mol Cell Biol **5:** 971–982

Nishida I, Murata N (1996) Chilling sensitivity in plants and cyanobacteria: The crucial contribution of membrane lipids. Annu Rev Plant Physiol Plant Mol Biol **47:** 541–568

Niyogi KK (1999) Photophotoprotection revisited: Genetic and molecular approaches. Annu Rev Plant Physiol Plant Mol Biol **50:** 333–359

Nolen B, Taylor S, Ghosh G (2004) Regulation of protein kinases; Controlling activity through activation segment conformation. Mol Cell **15:** 661–675

Oxborough K, Lee P, Horton P (1987) Regulation of thylakoid protein phosphorylation by high-energy-state quenching. FEBS Lett **221:** 211–214

Papageorgiou GC, Govindjee (2011) Photosystem II fluorescence: Slow changes—Scaling from the past. J Photochem Photobiol B **104:** 258–270

Pettersen EF, Goddard TD, Huang CC, Couch GS, Greenblatt DM, Meng EC, Ferrin TE (2004) UCSF Chimera—A visualization system for exploratory research and analysis. J Comput Chem **25:** 1605–1612

Pocock TH, Lachance MA, Pröschold T, Priscu JC, Kim SS, Hüner NPA (2004) Identification of psychrophilic green alga from Lake Bonney, Antarctica: *Chlamydomonas raudensis* Ettl. (UWO 241) *Chlorophyceae*. J Phycol **40:** 1138–1148

Pocock TH, Koziak A, Rosso D, Falk S, Hüner NPA (2007) *Chlamydomonas raudensis* (UWO 241), Chlorophyceae, exhibits the capacity for rapid d1 repair in response to chronic photoinhibition at low temperature. J Phycol **43:** 924–936

Possmayer M, Berardi G, Beall BFN, Trick CG, Hüner NPA, Maxwell DP (2011) Plasticity of the psychrophilic green alga *Chlamydomonas raudensis* (UWO 241) (Chlorophyta) to supraoptimal temperature stress. J Phycol **47:** 1098–1109

Possmayer M, Gupta RK, Szyszka-Mroz B, Maxwell DP, Lachance M-A, Hüner NPA, Smith DR (2016) Resolving the phylogenetic relationship between *Chlamydomonas sp*. UWO 241 and *Chlamydomonas raudensis* sag 49.72 (Chlorophyceae) with nuclear and plastid DNA sequences. J Phycol **52:** 305–310

Priscu JC, Fritsen CH, Adams EE, Giovannoni SJ, Paerl HW, McKay CP, Doran PT, Gordon DA, Lanoil BD, Pinckney JL (1998) Perennial Antarctic lake ice: An oasis for life in a polar desert. Science **280:** 2095–2098

Rochaix JD (2011) Reprint of: Regulation of photosynthetic electron transport. Biochim Biophys Acta **1807:** 878–886

Rochaix JD (2014) Regulation and dynamics of the light-harvesting system. Annu Rev Plant Biol **65:** 287–309

Ruban AV (2016) Nonphotochemical chlorophyll fluorescence quenching: Mechanism and effectiveness in protecting plants from photodamage. Plant Physiol **170:** 1903–1916

Salehian O, Bruce D (1992) Distribution of excitation energy in photosynthesis: Quantification of fluorescence yields from intact cyanobacteria. J Lumin **51:** 91–98

Samson G, Bruce D (1995) Complementary changes in absorption cross-sections of photosystems I and photosystems II due to phosphorylation and Mg^{2+}-depletion in spinach thylakoids. Biochim Biophys Acta **1232:** 21–26

Shapiguzov A, Chai X, Fucile G, Longoni P, Zhang L, Rochaix J-D (2016) Activation of the Stt7/STN7 kinase through dynamic interactions with the Cytochrome b_6f complex. Plant Physiol **171:** 82–92

Siddiqui KS, Williams TJ, Wilkins D, Yau S, Allen MA, Brown MV, Lauro FM, Cavicchioli R (2013) Psychrophiles. Annu Rev Earth Planet Sci **41:** 87–115

Sievers F, Wilm A, Dineen D, Gibson TJ, Karplus K, Li W, Lopez R, McWilliam H, Remmert M, Söding J, et al (2011) Fast, scalable generation of high-quality protein multiple sequence alignments using Clustal Omega. Mol Syst Biol **7:** 539

Slavov C, Reus M, Holzwarth AR (2013) Two different mechanisms cooperate in the desiccation-induced excited state quenching in *Parmelia* lichen. J Phys Chem B **117:** 11326–11336

Slavov C, Schrameyer V, Reus M, Ralph PJ, Hill R, Büchel C, Larkum AWD, Holzwarth AR (2016) "Super-quenching" state protects *Symbiodinium* from thermal stress—Implications for coral bleaching. Biochim Biophys Acta **1857:** 840–847

Spigel RH, Priscu JC (1996) Evolution of temperature and salt structure of Lake Bonney, a chemically stratified Antarctic lake. Hydrobiologia **321:** 177–190

Szyszka B, Ivanov AG, Hüner NPA (2007) Psychrophily is associated with differential energy partitioning, photosystem stoichiometry and polypeptide phosphorylation in *Chlamydomonas raudensis*. Biochim Biophys Acta **1767:** 789–800

Szyszka-Mroz B, Pittock P, Ivanov AG, Lajoie G, Hüner NPA (2015) The Antarctic psychrophile *Chlamydomonas* sp. UWO241 preferentially phosphorylates a photosystem I-cytochrome b_6/f supercomplex. Plant Physiol **169:** 717–736

Takahashi H, Iwai M, Takahashi Y, Minagawa J (2006) Identification of the mobile light-harvesting complex II polypeptides for state transitions in *Chlamydomonas reinhardtii*. Proc Natl Acad Sci USA **103:** 477–482

Takizawa K, Takahashi S, Hüner NPA, Minagawa J (2009) Salinity affects the photoacclimation of *Chlamydomonas raudensis* Ettl UWO241. Photosynth Res **99:** 195–203

Tikkanen M, Aro E-M (2012) Thylakoid protein phosphorylation in dynamic regulation of photosystem II in higher plants. Biochim Biophys Acta **1817:** 232–238

Tikkanen M, Aro E-M (2014) Integrative regulatory network of plant thylakoid energy transduction. Trends Plant Sci **19:** 10–17

Ueno Y, Aikawa S, Kondo A, Akimoto S (2016) Energy transfer in cyanobacteria and red algae: Confirmation of spillover in intact megacomplexes of phycobilisome and both photosystems. J Phys Chem Lett **7:** 3567–3571

Ünlü C, Drop B, Croce R, van Amerongen H (2014) State transitions in *Chlamydomonas reinhardtii* strongly modulate the functional size of photosystem II but not of photosystem I. Proc Natl Acad Sci USA **111:** 3460–3465

Vener A (2008) Phosphorylation of thylakoid proteins. *In* B Demmig-Adams, W Adams, A Mattoo, eds, Photoprotection Phototinhibition Gene Regulation and Environment, Springer, Dordrecht, the Netherlands, pp 107–126.

Vincent WF, Mueller D, van Hove P, Howard-Williams P (2004) Glacial periods on early Earth and implications for the evolution of life. *In* J Seckbach, ed, Cellular Origin, Life in Extreme Habitats and Astrobiology: Life As We Know It. Springer, Dordrecht, the Netherlands, pp 481–501

Wada H, Gombos Z, Sakamoto T, Murata N (1993) Role of lipids in low temperature adaptation. *In* HY Yamomoto and CM Smith,, eds, Photosynthetic Responses to the Environment, Vol **8**. American Society Plant Physiology, Bethsada, Maryland, pp 78–87

Wollman F-A, Diner BA (1980) Cation control of fluorescence emission, light scatter, and membrane stacking in pigment mutants of *Chlamydomonas reinhardi.* Arch Biochem Biophys **201:** 646–659

Wunder T, Liu Q, Aseeva E, Bonardi V, Leister D, Pribil M (2013) Control of *STN7* transcript abundance and transient STN7 dimerisation are involved in the regulation of STN7 activity. Planta **237:** 541–558

Xavier JC, Brandt A, Ropert-Coudert Y, Badhe R, Gutt J (2016) Future challenges in Southern Ocean ecology research. Front Mar Sci **3:** 94

Zer H, Ohad I (2003) Light, redox state, thylakoid-protein phosphorylation and signaling gene expression. Trends Biochem Sci **28:** 467–470